

P450-Catalyzed Intramolecular sp^3 C–H Amination with Arylsulfonyl Azide Substrates

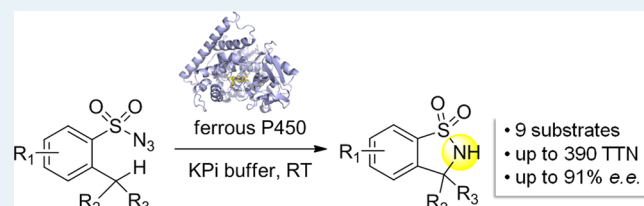
Ritesh Singh, Melanie Bordeaux, and Rudi Fasan*

Department of Chemistry, University of Rochester, Rochester, NY 14627

S Supporting Information

ABSTRACT: The direct amination of aliphatic C–H bonds represents a most valuable transformation in organic chemistry. While a number of transition-metal-based catalysts have been developed and investigated for this purpose, the possibility to execute this transformation with biological catalysts has remained largely unexplored. Here, we report that cytochrome P450 enzymes can serve as efficient catalysts for mediating intramolecular benzylic C–H amination reactions in a variety of arylsulfonyl azide compounds. Under optimized conditions, the P450 catalysts were found to support up to 390 total turnovers leading to the formation of the desired sultam products with excellent regioselectivity. In addition, the chiral environment provided by the enzyme active site allowed for the reaction to proceed in a stereo- and enantioselective manner. The C–H amination activity, substrate profile, and enantio/stereoselectivity of these catalysts could be modulated by utilizing enzyme variants with engineered active sites.

KEYWORDS: cytochrome P450, C–H amination, enzymatic catalysis, protein engineering, arylsulfonyl azides, sultams



1. INTRODUCTION

Catalytic methods for the direct amination of aliphatic (sp^3) C–H bonds are of outstanding synthetic relevance owing to the ubiquitous occurrence of amine functionalities among natural and synthetic molecules. In recent years, notable progress has been made in the development of transition-metal-based catalysts for the formation of C–N bonds, in particular through mechanisms involving metal–nitrenoid C–H insertion reactions.^{1–3} For example, efficient catalytic systems have been developed for this purpose that rely on Rh,^{4–7} Ir,^{8,9} Ru,¹⁰ Fe,¹¹ or Ag¹² complexes in combination with various nitrene sources (e.g., pre- or in situ-formed iminoiodinanes, azides). Following the pioneering work of Breslow and Gellman,¹³ other groups have also demonstrated the reactivity of metal–porphyrin complexes toward supporting the catalytic amination of aliphatic C–H bonds in both intra- and intermolecular settings.^{14–17}

While the toolbox of chemical strategies for C–H amination have continued to expand over the past decade, including notable enantioselective variations thereof,^{7,9,10,18,19} a biocatalytic counterpart in the natural world has thus far not been identified (i.e., an enzyme that can catalyze the formation of C–N bonds via the direct insertion of nitrene species into a saturated C–H bond). Indeed, known classes of enzymes implicated in C–N bond-forming transformations include ammonia lyases, aminomutases, and transaminases,^{20–23} all of which operate at carbon atom centers at higher oxidation states. Clearly, the development of enzymatic platforms for supporting C–H amination transformations would be very attractive, particularly toward the design and implementation of

sustainable and environmentally friendly procedures for chemical synthesis.²⁴

Of particular relevance to the present work is an early report from Dawson and Breslow,²⁵ which described the formation of a C–H amination product upon incubation of iminoiodane substrates with microsomal P450s in the ferric state. However, this catalytic activity was detected only at basal levels (0.6–2.2 turnovers), and no further investigations in this area have appeared in the literature over the following three decades. In addition, compared to organic azides, iminoiodinanes are less attractive as nitrene sources due to their poor atom economy. Here, we report that cytochrome P450s constitute efficient catalysts for supporting the formation of cyclic amines via the intramolecular C–H amination of arylsulfonyl azides. Notably, Arnold and co-workers have very recently described a similar reactivity for serine-ligated P450s (called P411s).²⁶ Complementing and extending beyond this work, the present study demonstrates that cysteine-ligated P450s are efficient catalysts for the C–H amination of arylsulfonyl azides and it provides first-time insights into the interplay of both electronic and steric factors in affecting such reactivity. In addition, the present work puts forth a mechanistic hypothesis that can explain the formation of the amination products and byproducts from these P450-catalyzed transformations, and building on the latter, it defines initial mutagenesis strategies for enhancing the C–H amination efficiency of these catalysts.

Received: October 9, 2013

Revised: November 27, 2013

2. EXPERIMENTAL SECTION

2.1. Reagents and Substrates. All solvents and reagents were purchased from commercial suppliers (Sigma-Aldrich, ACS Scientific, Acros) and used without any further purification, unless stated otherwise. The compound 2,4,6-triisopropylsulfonyl azide (**1a**) was purchased, whereas the other arylsulfonyl azides (**2a**, **3a**, **4–9**) were synthesized according to the procedures provided in the Supporting Information. Silica gel chromatography purifications were carried out using AMD silica gel 60 230–400 mesh. Preparative thin-layer chromatography was performed on TLC plates (Merck).

2.2. Protein Expression and Purification. P450s were expressed from pCWori-based plasmids containing the P450 gene under the control of a double *tac* promoter (*Bam*H I/*Eco*R I cassette), as described previously.²⁷ Typically, cultures of recombinant DH5 α cells in Terrific Broth (TB) medium (ampicillin, 100 mg L⁻¹) were grown at 37 °C (200 rpm) until the OD₆₀₀ reached 1.0, and they were then induced with 0.25 mM β -D-1-thiogalactopyranoside (IPTG) and 0.3 mM δ -aminolevulinic acid (ALA). After induction, cultures were shaken at 150 rpm and 27 °C and harvested after 20 h by centrifugation at 4000 rpm at 4 °C. Cells lysates were prepared by sonication and loaded on a Q resin column. The protein was eluted using 20 mM Tris, 340 mM NaCl, pH 8.0. After buffer exchange (50 mM potassium phosphate buffer, pH 8.0), the enzymes were stored at -80 °C. P450 concentration was determined from CO-binding difference spectra ($\epsilon_{450-490} = 91\,000\text{ M}^{-1}\text{ cm}^{-1}$). The vector encoding for the thermostable phosphite dehydrogenase (PTDH) variant Opt13 was kindly provided by the Zhao group.⁶ PTDH was overexpressed from the pET-15b-based vector in BL21(DE3) cells and purified using Ni-affinity chromatography according to the published procedure.²⁷

2.3. Enzymatic Reactions. The enzymatic reactions were carried out at a 400 μ L scale using 20 μ M P450, 10 mM substrate, and 10 mM sodium dithionite. In a typical procedure, a solution containing sodium dithionite (100 mM stock solution) in potassium phosphate buffer (50 mM, pH 8.0) was degassed by bubbling argon into the mixture for 5 min in a sealed vial. A buffered solution containing the P450 enzyme was carefully degassed in a similar manner in a separate vial. The two solutions were then mixed together via cannulation. Reactions were initiated by addition of 8 μ L of azide (from a 0.5 M stock solution in methanol) with a syringe, and the reaction mixture was stirred for 16 h at room temperature, under positive argon pressure. Reactions with NADPH as the reductant were conducted following an identical procedure with the exception that sodium dithionite was replaced with an NADPH solution in potassium phosphate buffer (final concentration: 5 or 10 mM). Reactions with hemin were carried out using an identical procedure with the exception that the purified P450 was replaced with 80 μ L of a hemin solution (100 μ M in DMSO/H₂O, 1:1). The large-scale reaction was carried out at 20 mL scale using degassed phosphate buffer containing a cofactor regeneration system (0.5 mM PTDH, 1 mM NADPH, 50 mM sodium phosphite), 30 mg of **3a**, and purified FL#62 at a final concentration of 40 μ M.

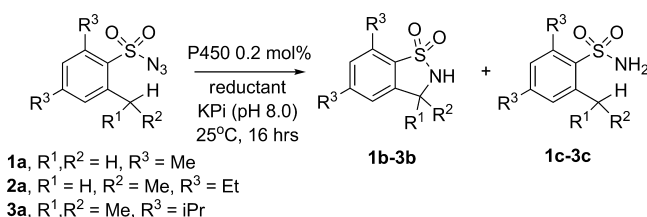
2.4. Product Analysis. The reactions were analyzed by adding 20 μ L of a guaiacol internal standard solution (80 mM in methanol) to the reaction mixture, followed by extraction with 400 μ L of dichloromethane (DCM). The organic layer

was removed via evaporation under reduced pressure. The residue was resuspended in 20 μ L of DCM, and the products as well as the internal standard were separated by preparative thin-layer chromatography (TLC, 30% EtOAc in hexane). From the TLC plates, all the products (and internal standard) were collected and extracted with 100 μ L of DCM. The resulting solutions were then analyzed by GC-FID or GC-MS (see below). Calibration curves of the different sultams were constructed using synthetically produced sultams and the internal standard (Figure S3). All measurements were performed at least in duplicate. For each experiment, negative control samples containing either no enzyme or no reductant were included. For the heat-inactivation experiments, the enzyme was preheated at 65 °C for 10 min prior to use. For the CO-inactivation experiment, carbon monoxide was bubbled through the reaction mixture containing the P450 enzyme and sodium dithionite prior to addition of the azide substrate. For enantio- and stereoselectivity determination, the samples were analyzed by supercritical fluid chromatography (see below). Authentic standards of racemic (\pm)-**2b** and (\pm)-**7b** were synthesized as described in the Supporting Information and used for calibration.

2.5. Analytical Methods. Gas chromatography (GC) analyses were carried out using a Shimadzu GC-2010 gas chromatograph equipped with a FID detector and a Shimadzu SHRXI-SMS column (15 m \times 0.25 mm \times 0.25 μ m film). Separation method: 1 μ L injection; injector temp: 250 °C; detector temp: 220 °C. Gradient: column temperature set at 60 °C for 1 min, then to 200 °C at 10 °C/min, then to 290 °C at 30 °C/min. Total run time was 19.00 min. GC/MS analyses were performed on a Shimadzu GCMS-QP2010 equipped with a RTX-XLB column (30 m \times 0.25 mm \times 0.28 μ m) and a quadrupole mass analyzer. Separation method: 5 μ L injection; inj. temp: 250 °C; detector temp: 220 °C. Gradient: column temperature set at 60 °C for 1 min, then to 320 °C at 30 °C/min, then to 320 °C for 4 min. Total run time was 13.67 min. Enantiomeric excess was determined by supercritical fluid chromatography (JESCO SF-2000) using a Chiralpak IA chiral column (4.6 m i.d. \times 250 mm) and a mixture of CO₂/isopropanol (75:25) as the mobile phase. Total run time: 10.2 min.

3. RESULTS AND DISCUSSION

3.1. Intramolecular C–H Amination with 2,4,6-Trialkyl-benzenesulfonyl Azides. Our studies began by testing the ability of cytochrome P450_{BM3}, a well-characterized and highly evolvable catalytically self-sufficient P450 system from *B. megaterium*,^{28–30} to perform the desired intramolecular C–H amination reaction in the presence of a series of 2,4,6-trisubstituted benzenesulfonyl azides (**1a–3a**, Table 1). Excitingly, successful conversion of 2,4,6-triethyl-benzenesulfonyl azide (**2a**) and 2,4,6-triisopropyl-benzenesulfonyl azide (**3a**) to the desired benzosultam products (**2b–3b**) could be achieved under anaerobic conditions in the presence of 0.2 mol % purified enzyme and sodium dithionite (Na₂S₂O₄, 10 mM). Under these conditions, P450_{BM3} exhibits only modest activity on **2a** (5 total turnovers (TTN)) but appreciable catalytic C–H amination activity with **3a** (20 TTN), the latter being about twice as high as that observed with free hemin (12 TTN). In contrast, no detectable amount of the desired cyclic amine was produced in both the enzymatic and hemin reaction with **1**. Subsequent experiments indicated that the P450-mediated conversion of **3a** (and **2a**) can be also

Table 1. C–H Amination Activity of P450_{BM3} Variants on 2,4,6-Trialkyl-benzenesulfonyl Azides^a

catalyst	product	TTN	product	TTN	product	TTN
hemin	1b	0	2b	2	3b	12
P450 _{BM3}	1b	0	2b	5 (5) ^b	3b	20 (15) ^b
139-3	1b	0	2b	6	3b	16
J	1b	0	2b	17	3b	51
FL#62	1b	5	2b	47	3b	388

^aReactions conditions: 20 μM P450, 10 mM azide, 10 mM Na₂S₂O₄. Total turnover numbers (TTN) were measured by GC from duplicate experiments (SD within 20%). See SI for details. ^bIn the presence of NADPH (10 mM) as reductant.

promoted by NADPH (10 mM), albeit with somewhat lower catalytic efficiency (15 TTN). Omission of either reductant (i.e., sodium dithionite or NADPH) from the reaction mixture resulted in no product formation, indicating that the ferrous P450 is the catalytically active form of the enzyme. The presence of air in the reaction vessel also completely suppressed the P450-dependent C–H amination activity.

In addition to the C–H amination products, the reactions with **2a** and **3a** also led to accumulation of 2,4,6-triisopropyl-(**3c**) and 2,4,6-triethyl-benzenesulfonamide (**2c**), respectively, as byproducts. As determined via control experiments, NADPH, unlike dithionite, is unable to reduce these azides to the corresponding sulfonamides. Thus, accumulation of the latter in the NADPH-supported reactions indicated that this species constitutes a product of the enzymatic reaction as well, likely resulting from unproductive decomposition of the iron–nitrene intermediate as discussed later. Additional control experiments were performed in the presence of **3a** and using either CO-saturated buffer or heat-denatured P450_{BM3}, both of which were expected to irreversibly inactivate the enzyme. Observation of no or negligible amounts of the sultam **3b** or sulfonamide **3c** unequivocally confirmed the direct involvement of the protein-coordinated heme and properly folded P450, respectively, for the observed catalytic C–H amination activity.

3.2. Engineered P450_{BM3} Variants. Encouraged by these results, we extended our studies to include a set of engineered P450_{BM3}-derived variants, namely, 139–3,³¹ J,³² and FL#62,²⁷ which carry multiple (2 to 6) active-site mutations compared to the parent enzyme (Table S1). These variants were chosen on the basis of their higher oxidation activity across a variety of bulky, non-native substrates, as determined in previous studies.^{27,33,34} These features suggested that these enzymes possess an enlarged active site, which could thus better accommodate compounds **1a–3a** as well as additional substrates tested later. Gratifyingly, these engineered P450 variants, and in particular FL#62, were found to exhibit enhanced C–H amination activity (Table 1). Most notably, FL#62 was determined to support 10- and 20-fold higher total turnovers for the cyclization of **2a** (47 TTN) and **3a** (388 TTN), respectively, compared to P450_{BM3}. In addition, FL#62 also showed detectable C–H amination activity (5 TTN) on the compound with the least-activated benzylic C–H bond

within this substrate series (i.e., 2,4,6-trimethylbenzenesulfonyl azide (**1a**)). In each case, the P450-catalyzed C–H amination reactions with **2a** and **3a** were found to proceed with absolute regioselectivity toward activation of the benzylic position in the substrate, thus resulting in the corresponding 5-membered lactam rings. Another interesting observation concerns the order of reactivity of all these P450s toward this set of structurally related substrates, namely, **1a** ≪ **2a** ≪ **3a** (Table 1). This trend can be in part explained on the basis of the decreasing bond dissociation energy associated with the benzylic C–H bond, making it increasingly more reactive toward P450-catalyzed C–H nitrene insertion. Other factors, however, contribute to influence the reactivity of these catalysts as evidenced by subsequent studies.

3.3. Investigation of Substrate Scope. To further explore the substrate scope of these P450-based C–H amination catalysts, additional substrates were synthesized (see Supporting Information for details) and tested. A first group of compounds comprised both unsubstituted and substituted arylsulfonyl azides, containing a single isopropyl moiety in *ortho* to the sulfonyl azido group (**4–6**, Figure 1A). With 2-isopropylbenzene sulfonyl azide **4**, only FL#62 shows detectable C–H amination activity (TTN: 5). Interestingly, the introduction of a bulky substituent (–*i*Pr, –CO₂Me) in position 4 of the aromatic ring (**5**, **6**) resulted in more efficient conversion to the desired C–H amination products, **5b** and **6b**, respectively, by all the enzymes and in particular by FL#62 (Figure 1B). With the latter, TTN values in the range of 15–25 could be achieved. Although these catalytic activities remain significantly (10- to 20-fold) lower than those observed with **3a**, they compare favorably with those obtained using Ir- and Co-based catalysts on similar substrates (30–50 TTN).^{9,16} To examine the impact of steric influences at the level of the 2-alkyl moiety, compounds **7–9** were subsequently prepared and tested. Whereas only minimal conversion to the desired cyclic amines (i.e., 1–2 TTN) were observed in the presence of the more sterically demanding **8** and **9**, much higher C–H amination activity was obtained with **7** and the engineered P450_{BM3} variants, with FL#62 supporting over 190 TTN on this substrate (Figure 1A, Table S2).

Although saturating substrate concentrations (10 mM) were used in the reactions above, we wondered whether differences in substrate accessibility to the enzyme active site could account for the variation in the C–H amination product yields observed in these experiments. Repeating the reactions with FL#62 and **4–9** in the presence of NADPH revealed that in addition to the cyclic amines, the corresponding arylsulfonamide byproducts were produced in each case (Figure S1). These results clearly indicated that all the substrates, including **8** and **9**, could access the heme cofactor within the FL#62 active site. The sultam/sulfonamide ratio, however, varied significantly across the different substrates (Figure S1). Collectively, these experiments suggested that additional factors, besides the electronic effects mentioned above, strongly influence whether the P450-catalyzed reaction proceeds through a productive pathway, leading to the C–H amination product, versus a nonproductive one, leading to the reduced sulfonamide.

3.3. Proposed Mechanism for C–H Amination Reaction. A possible mechanism for the P450-catalyzed C–H amination reaction is provided in Scheme 1, as formulated on the basis of our results and previous studies with metalloporphyrins^{35–39} and nonheme iron systems.^{40–43} We envision that interaction of the azide substrate with the ferrous

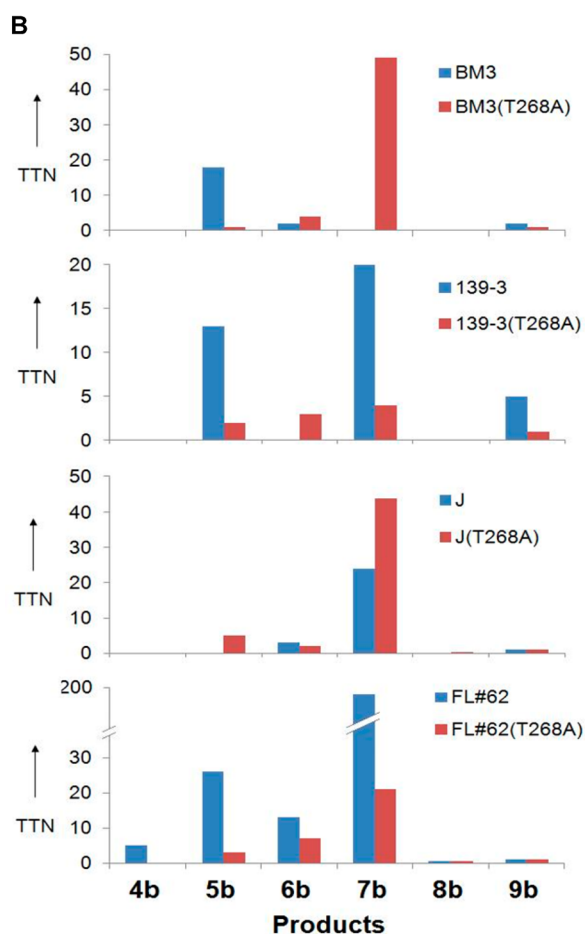
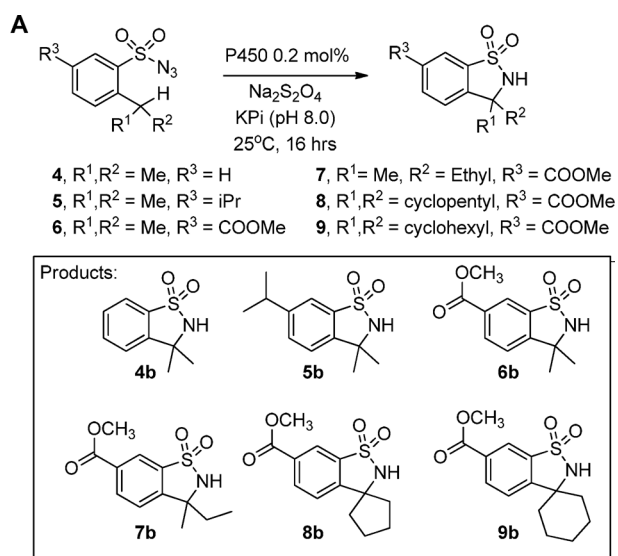
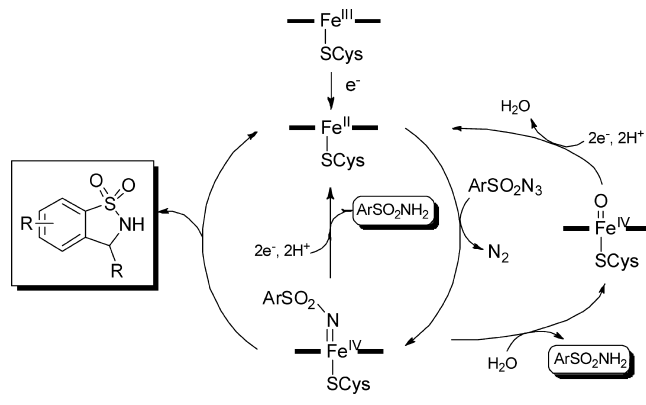


Figure 1. Substrate scope of P450 C–H amination catalysts. (A) Tested substrates and corresponding benzosultam products. (B) Measured TTNs for the different P450 variants (see also Table S2).

heme center in the P450 forms an initial azido–iron(II) complex, which ultimately leads to the formation of an imido–iron(IV) species ((heme)Fe^{IV} = N=O₂Ar) via extrusion of N₂. In a productive pathway, this reactive intermediate would then engage the neighboring benzylic site in a nitrene C–H bond insertion reaction (via a stepwise hydrogen-atom abstraction/radical rebound or a concerted process) to give the cyclic

Scheme 1. Proposed Mechanism for the Formation of the Benzosultam and Benzosulfonamide Products in the P450-Catalyzed Reactions



amine. The P450-dependent formation of the reduced arylsulfonamide also suggest competition from a nonproductive pathway leading to this byproduct. Conceivably, this species could be formed via direct reduction of the imido–iron(IV) intermediate. Since water exchange at high-valent iron species in P450s has been documented,^{25,44–46} a parallel or alternative pathway could involve hydrolysis of the imido–iron(IV) intermediate followed by reduction of the resulting oxo–iron(IV) species to give the ferrous heme. Beside the fact that a ferrous heme was found to be essential for the observed C–H amination activity, additional evidence in support of this mechanistic hypothesis is our observation that stoichiometric amounts of NADPH (with respect to the P450) are sufficient to support catalysis (e.g., 18 TTN with FL#62 and 3a), but an excess of reducing equivalents is required for supporting much higher total turnover numbers (189 TTN with 250 equiv NADPH), possibly due to these competing electron-consuming pathways.

The observed structure–reactivity trends across the various arylsulfonyl azide substrates also deserve further comment. Particularly intriguing are: (i) the large difference between the catalytic performance of the enzymes with 7 versus 6 (e.g., FL#62: 192 vs 13 TTN, Table S2), which differ merely by a single methyl group at the level of the 2-alkyl chain; and (ii) the beneficial effect of the more remote *meta* substitutions in the benzene ring toward increasing the amount of sultam product with substrates 5 and 6 as compared to 4 (Figure 1). As noted earlier, our experiments indicate that all of these substrates are able to access the heme in FL#62, although only 5, 6, and 7 undergo efficient C–H amination (Figure S1). Unlike the 1a–3a series, the structural differences within this set of related substrates are not expected to have a major effect on the inherent reactivity of the benzylic C–H bond. At the same time, they are likely to affect the relative orientation of the putative imido–iron(IV) intermediate within the enzyme active site (Scheme 1). Thus, a possible explanation for these results may be linked to the ability of these substituents to favor a conformation of such intermediate that favors nitrene insertion into the benzylic C–H bond over a nonproductive one leading to the sulfonamide product. In this regard, it is instructive to note how the substituents –COOMe (in 6) and –CH(CH₃)₂ (in 5), which have opposite electronic but similar steric demands, lead to very similar benzosultam-to-sulfonamide ratios (6.5% vs 5.5%, Figure S1).

3.4. T268A Mutation. While further studies are ongoing to validate the mechanistic hypotheses outlined above, an implication of our proposed mechanism is that protonation of the imido–iron(IV) intermediate may be responsible for the formation of the undesired sulfonamide byproduct. In P450_{BM3}, a highly conserved threonine residue (Thr268), which is located within the I-helix in close proximity of the heme (Figure 2),^{47,48} is intimately involved in the protonation/

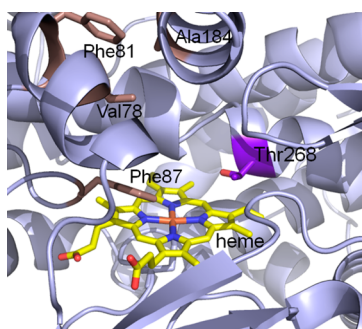


Figure 2. Close-up view of the active site cavity in the substrate-bound structure of P450_{BM3} (pdb 1FAG⁴⁸). The heme cofactor and Thr268 residue are highlighted in yellow and purple, respectively. Active-site positions that are mutated in the P450 variants tested in this study are also labeled (brown, see Table S1). The enzyme-bound substrate (palmitate) and part of the protein structure are not shown for clarity.

stabilization of heme-bound intermediates (e.g., hydroperoxy–iron species) during the catalytic cycle of P450s as monooxygenases.^{49,50} Accordingly, a T268A mutation was introduced by site-directed mutagenesis into wild type P450_{BM3} and each of the variants in an attempt to improve the C–H amination activity of these enzymes. Side-by-side comparison of the catalytic performance of the T268A variants with the corresponding parent enzymes revealed clear beneficial effects resulting from the T268A mutation in the context of the P450-catalyzed nitrene transfer reactions investigated here, although a certain dependence on the nature of the parent enzyme and substrate was also observed (Figure 1, Table S2). Indeed, this mutation led to a general increase in TTN for P450_{BM3}(T268A) and J(T268A) but also a lower TTN for 139-3(T268A) and FL#62(T268A), as compared to their respective parent enzymes. Interestingly, a consistent enhancement of C–H amination activity across all the enzymes was achieved as a result of the T268A substitution with 2,4,6-triethylbenzenesulfonyl azide (**2a**). Indeed, whereas P450_{BM3} shows modest C–H amination activity on **2a** (5 TTN), P450_{BM3}(T268A) was found to support more than 40 TTN on this substrate. Similarly, a 2- to 6-fold increase in TTN was observed also for the T268A-containing variants of 139-3, J, and FL#62 (Table S2).

To evaluate the impact of the mutation on the sultam versus sulfonamide ratio, reactions with these eight enzymes were repeated in the presence of **2a** as the substrate and NADPH as the reductant. For each pair, a significant reduction in the fraction of the reduced sulfonamide byproduct was observed as a result of the T268A substitution, as illustrated by the data in Figure S2. Altogether, these data are consistent with our hypothesis that the beneficial effect of this mutation may be linked to the suppression of deleterious protonation mechanisms during P450-supported C–H amination catalysis. In this regard, it is interesting to note that mutation of the Thr268 residue was also found to enhance the activity of P450_{BM3} and

engineered variants thereof, as carbene transfer catalysts,^{51,52} possibly via disruption of analogous nonproductive proton-transfer-dependent processes. In the future, it will be interesting to establish whether further improvements in the C–H amination efficiency of these enzymes can be achieved by targeting more remote amino acid residues involved in the proton relay pathway in P450_{BM3}.⁵³ For the time being, the differential performance of the various P450_{BM3} variants on the same substrate as described above and our results with the T268A variants provide a first demonstration of the possibility of modulating and enhancing the C–H amination activity of these P450-based catalysts by means of active-site mutagenesis.

3.5. Enantio- and Stereoselectivity of P450 C–H Amination Catalysts. Optically active benzosultams represent valuable synthetic intermediates, which find use, for example, as chiral auxiliaries.^{54–56} The heme pocket in P450 enzymes offers an inherently asymmetric environment, in which the C–H amination reaction could occur in an enantio- or stereoselective manner. To investigate this aspect, we evaluated the enantiomeric excess produced by the different P450_{BM3} variants in the presence of the prochiral substrate **2a** and the racemic substrate **7**, thereby assessing the degree of stereo- and enantioselectivity, respectively, exhibited by these catalysts. Notably, moderate to very good asymmetric induction was observed in most cases (Table 2). In the case of **7**,

Table 2. Stereo- and Enantioselectivity in the P450-Catalyzed Cyclization of **2a and **7****

catalyst	product	ee (%) ^a	product	ee (%) ^{a,b,c}
hemin	2b	0	7b	0
P450 _{BM3}	2b	18	7b	n.a.
P450 _{BM3} (T268A)	2b	38	7b	55
139-3	2b	63	7b	–66
139-3 (T268A)	2b	91	7b	–53
J	2b	15	7b	–16
J (T268A)	2b	86	7b	–5
FL#62	2b	50	7b	1
FL#62 (T268A)	2b	5	7b	47

^aDetermined by SFC (supercritical fluid chromatography) analysis using authentic racemic standards as reference (see SI for details). ^bn.a. = not active. ^cSign indicates whether one or the opposite enantiomer (neg. sign) is formed.

P450_{BM3}(T268A) and 139-3 showed the largest degree of enantioselectivity, also displaying enantiocomplementarity toward formation of the chiral sultam **7b** (55% and –66% ee, respectively). With **2a**, the highest stereoselectivity was achieved with 139-3(T268A), which produced the corresponding cyclic amine **2b** in an enantiomeric excess as high as 91%. Another noteworthy result was the dramatic improvement in stereoselectivity (15→86% ee) as a result of the single T268A mutation with P450 variant J and substrate **2a**. Thus, besides altering the sultam to sulfonamide ratio during conversion of **2a** as discussed above, this mutation can have also an impact on the stereoselectivity of the C–H nitrene insertion process, likely due to the subtle change of the active-site environment in

close proximity to the putative imido–iron intermediate of Scheme 1 (see also Figure 2). Clearly, further studies (e.g., via molecular modeling) will be required to better understand the effect of the active mutations on the stereo- and enantioselectivity of these enzymes, including the apparent context-dependent effect of the T268A mutation in either enhancing or decreasing such selectivity (Table 2). In the context of the present study, the aforementioned results prove the viability of these P450-based catalysts to execute asymmetric C–H amination reactions as well as the possibility to tune their enantio- and stereoselectivity via manipulation of their active site.

3.6. Scalability of P450-Catalyzed C–H Amination Reaction. Finally, a preparative-scale transformation was set up using 0.4 mol % FL#62, substrate **3a** (30 mg), and a phosphite dehydrogenase-based NADPH cofactor regeneration system.⁵⁷ From this reaction, benzosultam **3b** could be isolated in 42% yield, which provided a proof-of-principle demonstration of the scalability of these enzymatic reactions.

4. CONCLUSIONS

In summary, this work demonstrates the potential of cytochrome P450 enzymes to provide efficient catalysts for the intramolecular C–H amination of arylsulfonyl azide substrates. In the parallel work by McIntosh et al.,²⁶ it was proposed that substitution of the heme proximal ligand cysteine with serine is necessary for conferring P450s with C–H amination reactivity. The present study clearly shows that cysteine–heme-ligated P450s can support this chemical transformation with equal or even higher efficiency. Whether the C–H amination reactivity of the catalysts described here can be further enhanced and modulated by modification of the heme environment remains an open question which will be addressed in the future. Importantly, the present work further shows how the substrate scope, C–H amination activity, and enantio- and stereoselectivity of these catalysts could be effectively altered and tuned by utilizing different active-site enzyme variants and through protein engineering. In particular, building on preliminary hypotheses regarding the mechanism underlying this newly discovered reactivity of P450 enzymes, our results suggest that disrupting the native proton relay pathway in P450s can provide a route for enhancing the C–H amination efficiency of these catalysts. Further work is ongoing toward validating the proposed mechanism and further capitalizing on these initial findings.

Cytochrome P450 enzymes constitute attractive catalytic platforms for oxygen-atom transfer reactions.^{31,58–65} The present study expands the scope of these biocatalysts to include a most valuable nitrene transfer reactivity, which has so far remained undocumented for naturally occurring enzymes and restricted to synthetic transition-metal-based catalysts. As illustrated by notable recent examples,^{52,66} the possibility to leverage natural or artificial enzyme scaffolds for “non-native” chemical transformations is bound to disclose exciting, new opportunities toward their exploitation for synthetic applications.

■ ASSOCIATED CONTENT

Supporting Information

Experimental details, characterization data, and supplemental figures and tables. This material is available free of charge via the Internet at <http://pubs.acs.org>.

■ AUTHOR INFORMATION

Corresponding Author

*E-mail: fasan@chem.rochester.edu.

Notes

The authors declare no competing financial interest.

■ ACKNOWLEDGMENTS

We thank Prof. Frances H. Arnold for kindly providing plasmids encoding for 139-3 and J and Prof. Daniel J. Weix for providing access to and assistance with the SFC instrumentation. This work was supported by the U.S. National Institute of Health R01 grant GM098628. MS instrumentation was supported by the U.S. National Science Foundation grant CHE-0946653.

■ REFERENCES

- (1) Davies, H. M. L.; Manning, J. R. *Nature* **2008**, *451* (7177), 417–424.
- (2) Muller, P.; Fruit, C. *Chem. Rev.* **2003**, *103* (8), 2905–2919.
- (3) Collet, F.; Dodd, R. H.; Dauban, P. *Chem. Commun.* **2009**, *34*, 5061–5074.
- (4) Espino, C. G.; Du Bois, J. *Angew. Chem., Int. Ed.* **2001**, *40* (3), 598–600.
- (5) Fiori, K. W.; Fleming, J. J.; Du Bois, J. *Angew. Chem., Int. Ed.* **2004**, *43* (33), 4349–4352.
- (6) Espino, C. G.; Fiori, K. W.; Kim, M.; Du Bois, J. *J. Am. Chem. Soc.* **2004**, *126* (47), 15378–15379.
- (7) Liang, C.; Collet, F.; Robert-Peillard, F.; Muller, P.; Dodd, R. H.; Dauban, P. *J. Am. Chem. Soc.* **2008**, *130* (1), 343–350.
- (8) Sun, K.; Sachwani, R.; Richert, K. J.; Driver, T. G. *Org. Lett.* **2009**, *11* (16), 3598–3601.
- (9) Ichinose, M.; Suematsu, H.; Yasutomi, Y.; Nishioka, Y.; Uchida, T.; Katsuki, T. *Angew. Chem., Int. Ed.* **2011**, *50* (42), 9884–9887.
- (10) Milczek, E.; Boudet, N.; Blakey, S. *Angew. Chem., Int. Ed.* **2008**, *47* (36), 6825–6828.
- (11) Paradine, S. M.; White, M. C. *J. Am. Chem. Soc.* **2012**, *134* (4), 2036–2039.
- (12) Cui, Y.; He, C. *Angew. Chem., Int. Ed.* **2004**, *43* (32), 4210–4212.
- (13) Breslow, R.; Gellman, S. H. *J. Chem. Soc. Chem. Comm.* **1982**, *24*, 1400–1401.
- (14) Yu, X. Q.; Huang, J. S.; Zhou, X. G.; Che, C. M. *Org. Lett.* **2000**, *2* (15), 2233–2236.
- (15) Cenini, S.; Gallo, E.; Penoni, A.; Ragaini, F.; Tollari, S. *Chem. Commun.* **2000**, *22*, 2265–2266.
- (16) Ruppel, J. V.; Kamble, R. M.; Zhang, X. P. *Org. Lett.* **2007**, *9* (23), 4889–4892.
- (17) Jin, L. M.; Xu, X.; Lu, H.; Cui, X.; Wojtas, L.; Zhang, X. P. *Angew. Chem., Int. Ed.* **2013**, *52* (20), 5309–5313.
- (18) Reddy, R. P.; Lee, G. H.; Davies, H. M. L. *Org. Lett.* **2006**, *8* (16), 3437–3440.
- (19) Zalatan, D. N.; Du Bois, J. *J. Am. Chem. Soc.* **2008**, *130* (29), 9220–9221.
- (20) Turner, N. J. *Curr. Opin. Chem. Biol.* **2011**, *15* (2), 234–240.
- (21) Bommarius, A. S.; Blum, J. K.; Abrahamson, M. J. *Curr. Opin. Chem. Biol.* **2011**, *15* (2), 194–200.
- (22) Heberling, M. M.; Wu, B.; Bartsch, S.; Janssen, D. B. *Curr. Opin. Chem. Biol.* **2013**, *17* (2), 250–260.
- (23) de Villiers, M.; Puthan Veetil, V.; Raj, H.; de Villiers, J.; Poelarends, G. J. *ACS Chem. Biol.* **2012**, *7* (10), 1618–1628.
- (24) Bornscheuer, U. T.; Huisman, G. W.; Kazlauskas, R. J.; Lutz, S.; Moore, J. C.; Robins, K. *Nature* **2012**, *485* (7397), 185–194.
- (25) Svatits, E. W.; Dawson, J. H.; Breslow, R.; Gellman, S. H. *J. Am. Chem. Soc.* **1985**, *107*, 6427–6428.
- (26) McIntosh, J. A.; Coelho, P. S.; Farwell, C. C.; Wang, Z. J.; Lewis, J. C.; Brown, T. R.; Arnold, F. H. *Angew. Chem., Int. Ed.* **2013**, *52* (35), 9309–9312.

- (27) Zhang, K.; El Damaty, S.; Fasan, R. *J. Am. Chem. Soc.* **2011**, *133* (10), 3242–3245.
- (28) Lewis, J. C.; Coelho, P. S.; Arnold, F. H. *Chem. Soc. Rev.* **2011**, *40* (4), 2003–2021.
- (29) Fasan, R. *ACS Catal.* **2012**, *2* (4), 647–666.
- (30) Whitehouse, C. J.; Bell, S. G.; Wong, L. L. *Chem. Soc. Rev.* **2012**, *41* (3), 1218–1260.
- (31) Glieder, A.; Farinas, E. T.; Arnold, F. H. *Nat. Biotechnol.* **2002**, *20* (11), 1135–1139.
- (32) Peters, M. W.; Meinhold, P.; Glieder, A.; Arnold, F. H. *J. Am. Chem. Soc.* **2003**, *125* (44), 13442–13450.
- (33) Fasan, R.; Mehareenna, Y. T.; Snow, C. D.; Poulos, T. L.; Arnold, F. H. *J. Mol. Biol.* **2008**, *383* (5), 1069–1080.
- (34) Zhang, K. D.; Shafer, B. M.; Demars, M. D.; Stern, H. A.; Fasan, R. *J. Am. Chem. Soc.* **2012**, *134* (45), 18695–18704.
- (35) Groves, J. T.; Takahashi, T. *J. Am. Chem. Soc.* **1983**, *105* (7), 2073–2074.
- (36) Mansuy, D.; Battioni, P.; Mahy, J. P. *J. Am. Chem. Soc.* **1982**, *104* (16), 4487–4489.
- (37) Au, S. M.; Huang, J. S.; Yu, W. Y.; Fung, W. H.; Che, C. M. *J. Am. Chem. Soc.* **1999**, *121* (39), 9120–9132.
- (38) Fantauzzi, S.; Gallo, E.; Caselli, A.; Ragaini, F.; Casati, N.; Macchi, P.; Cenini, S. *Chem. Commun.* **2009**, *26*, 3952–3954.
- (39) Lyaskovskyy, V.; Suarez, A. I. O.; Lu, H. J.; Jiang, H. L.; Zhang, X. P.; de Bruin, B. J. *J. Am. Chem. Soc.* **2011**, *133* (31), 12264–12273.
- (40) Jensen, M. P.; Mehn, M. P.; Que, L. *Angew. Chem., Int. Ed.* **2003**, *42* (36), 4357–4360.
- (41) Eckert, N. A.; Vaddadi, S.; Stoian, S.; Lachicotte, R. J.; Cundari, T. R.; Holland, P. L. *Angew. Chem., Int. Ed.* **2006**, *45* (41), 6868–6871.
- (42) Lucas, R. L.; Powell, D. R.; Borovik, A. S. *J. Am. Chem. Soc.* **2005**, *127* (33), 11596–11597.
- (43) Klinker, E. J.; Jackson, T. A.; Jensen, M. P.; Stubna, A.; Juhasz, G.; Bominaar, E. L.; Munck, E.; Que, L., Jr. *Angew. Chem., Int. Ed.* **2006**, *45* (44), 7394–7397.
- (44) Heimbrook, D. C.; Sligar, S. G. *Biochem. Biophys. Res. Commun.* **1981**, *99* (2), 530–535.
- (45) Macdonald, T. L.; Burka, L. T.; Wright, S. T.; Guengerich, F. P. *Biochem. Biophys. Res. Commun.* **1982**, *104* (2), 620–625.
- (46) White, R. E.; Mccarthy, M. B. *J. Am. Chem. Soc.* **1984**, *106* (17), 4922–4926.
- (47) Yeom, H.; Sligar, S. G.; Li, H. Y.; Poulos, T. L.; Fulco, A. J. *Biochemistry* **1995**, *34* (45), 14733–14740.
- (48) Li, H.; Poulos, T. L. *Nat. Struct. Biol.* **1997**, *4* (2), 140–146.
- (49) Martinis, S. A.; Atkins, W. M.; Stayton, P. S.; Sligar, S. G. *J. Am. Chem. Soc.* **1989**, *111* (26), 9252–9253.
- (50) Denisov, I. G.; Makris, T. M.; Sligar, S. G.; Schlichting, I. *Chem. Rev.* **2005**, *105* (6), 2253–2277.
- (51) Coelho, P. S.; Brustad, E. M.; Kannan, A.; Arnold, F. H. *Science* **2013**, *339* (6117), 307–310.
- (52) Coelho, P. S.; Wang, Z. J.; Ener, M. E.; Baril, S. A.; Kannan, A.; Arnold, F. H.; Brustad, E. M. *Nat. Chem. Biol.* **2013**, *9* (8), 485–487.
- (53) Yeom, H. Y.; Sligar, S. G. *Arch. Biochem. Biophys.* **1997**, *337* (2), 209–216.
- (54) Oppolzer, W.; Wills, M.; Starkemann, C.; Bernardinelli, G. *Tetrahedron Lett.* **1990**, *31* (29), 4117–4120.
- (55) Oppolzer, W.; Wills, M.; Kelly, M. J.; Signer, M.; Blagg, J. *Tetrahedron Lett.* **1990**, *31* (35), 5015–5018.
- (56) Oppolzer, W.; Rodriguez, I.; Starkemann, C.; Walther, E. *Tetrahedron Lett.* **1990**, *31* (35), 5019–5022.
- (57) McLachlan, M. J.; Johannes, T. W.; Zhao, H. *Biotechnol. Bioeng.* **2008**, *99* (2), 268–274.
- (58) Xu, F.; Bell, S. G.; Lednik, J.; Insley, A.; Rao, Z.; Wong, L. L. *Angew. Chem., Int. Ed.* **2005**, *44* (26), 4029–4032.
- (59) Fasan, R.; Chen, M. M.; Crook, N. C.; Arnold, F. H. *Angew. Chem., Int. Ed.* **2007**, *46* (44), 8414–8418.
- (60) Li, S.; Chaulagain, M. R.; Knauff, A. R.; Podust, L. M.; Montgomery, J.; Sherman, D. H. *Proc. Natl. Acad. Sci. U.S.A.* **2009**, *106* (44), 18463–18468.
- (61) Lewis, J. C.; Mantovani, S. M.; Fu, Y.; Snow, C. D.; Komor, R. S.; Wong, C. H.; Arnold, F. H. *ChemBioChem* **2010**, *11* (18), 2502–2505.
- (62) Weber, E.; Seifert, A.; Antonovici, M.; Geinitz, C.; Pleiss, J.; Urlacher, V. B. *Chem. Commun.* **2011**, *47*, 944–946.
- (63) Zilly, F. E.; Acevedo, J. P.; Augustyniak, W.; Deege, A.; Hausig, U. W.; Reetz, M. T. *Angew. Chem., Int. Ed.* **2011**, *50* (12), 2720–2724.
- (64) Bordeaux, M.; Galarneau, A.; Fajula, F.; Drone, J. *Angew. Chem., Int. Ed.* **2011**, *50* (9), 2075–2079.
- (65) Rea, V.; Kolkman, A. J.; Vottero, E.; Stronks, E. J.; Ampt, K. A.; Honing, M.; Vermeulen, N. P.; Wijmenga, S. S.; Commandeur, J. N. *Biochemistry* **2012**, *51* (3), 750–760.
- (66) Hyster, T. K.; Knorr, L.; Ward, T. R.; Rovis, T. *Science* **2012**, *338* (6106), 500–503.

Supplementary Information for

P450-catalyzed intramolecular sp^3 C—H amination with arylsulfonyl azide substrates

Ritesh Singh, Melanie Bordeaux & Rudi Fasan*

Department of Chemistry, University of Rochester, 14627 Rochester, New York, USA

Correspondence should be addressed to R.F. (fasan@chem.rochester.edu)

Table of contents:

Supplementary Figure S1-S4	Pages S2-S6
Supplementary Table S1-S2	Pages S7-S8
Synthetic Procedures	Pages S9-S19
Spectral Data	Page S20-S47
References	Page S48

Figure S1: Product distribution for the reactions of FL#62 with substrates **1a-3a** and **4-9**. The bar graph describes the relative amount of the arylsultam and arylsulfonamide products generated in the reactions. Cumulative total turnover numbers (TTN) corresponding to both products are indicated. Reactions conditions: 20 μ M FL#62, 10 mM substrate, 5 mM NADPH. Reactions were carried out at room temperature and under argon, stopped after 16 hours, and analyzed by gas chromatography.

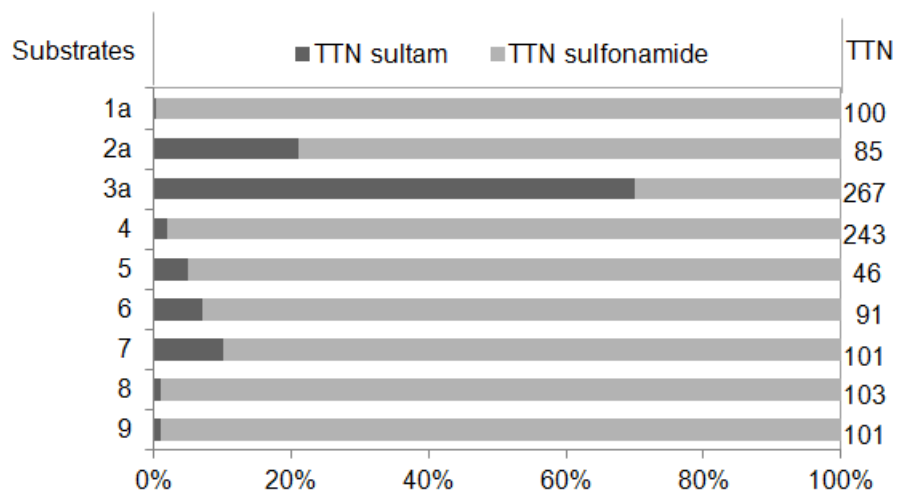


Figure S2: Percentage of C—H amination product (= [arylsultam] / ([arylsultam]+[arylsulfonamide])) from the reactions of P450_{BM3} (=WT), J, 139-3, FL#62 (light blue) and their T268A-containing counterparts (dark blue) with substrate **2a**. Reactions conditions: 20 μ M P450, 10 mM substrate, 5 mM NADPH. Reactions were carried out at room temperature and under argon, stopped after 16 hours, and analyzed by gas chromatography.

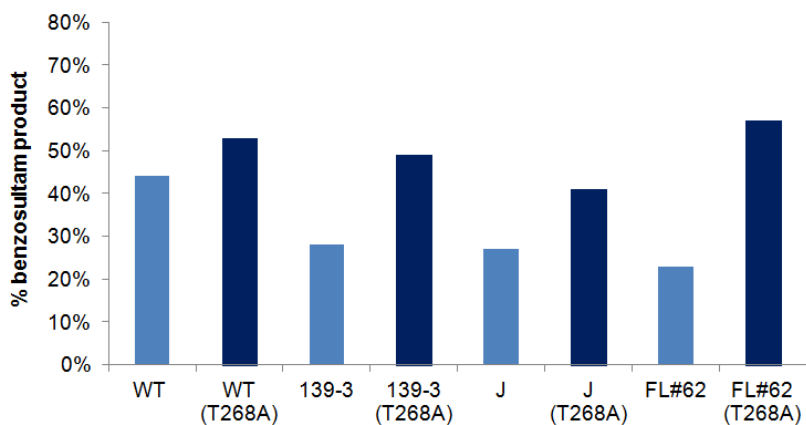


Figure S3. Calibration curves used for the quantification of the benzosultam products by GC-MS (2b, 8b, 9b) or GC-FID (1b, 3b, 4b, 5b, 6b, 7b). The graphs report the ratio between the peak areas corresponding to the benzosultam product (authentic standard prepared synthetically) and the internal standard (IS) plotted against the benzosultam concentration.

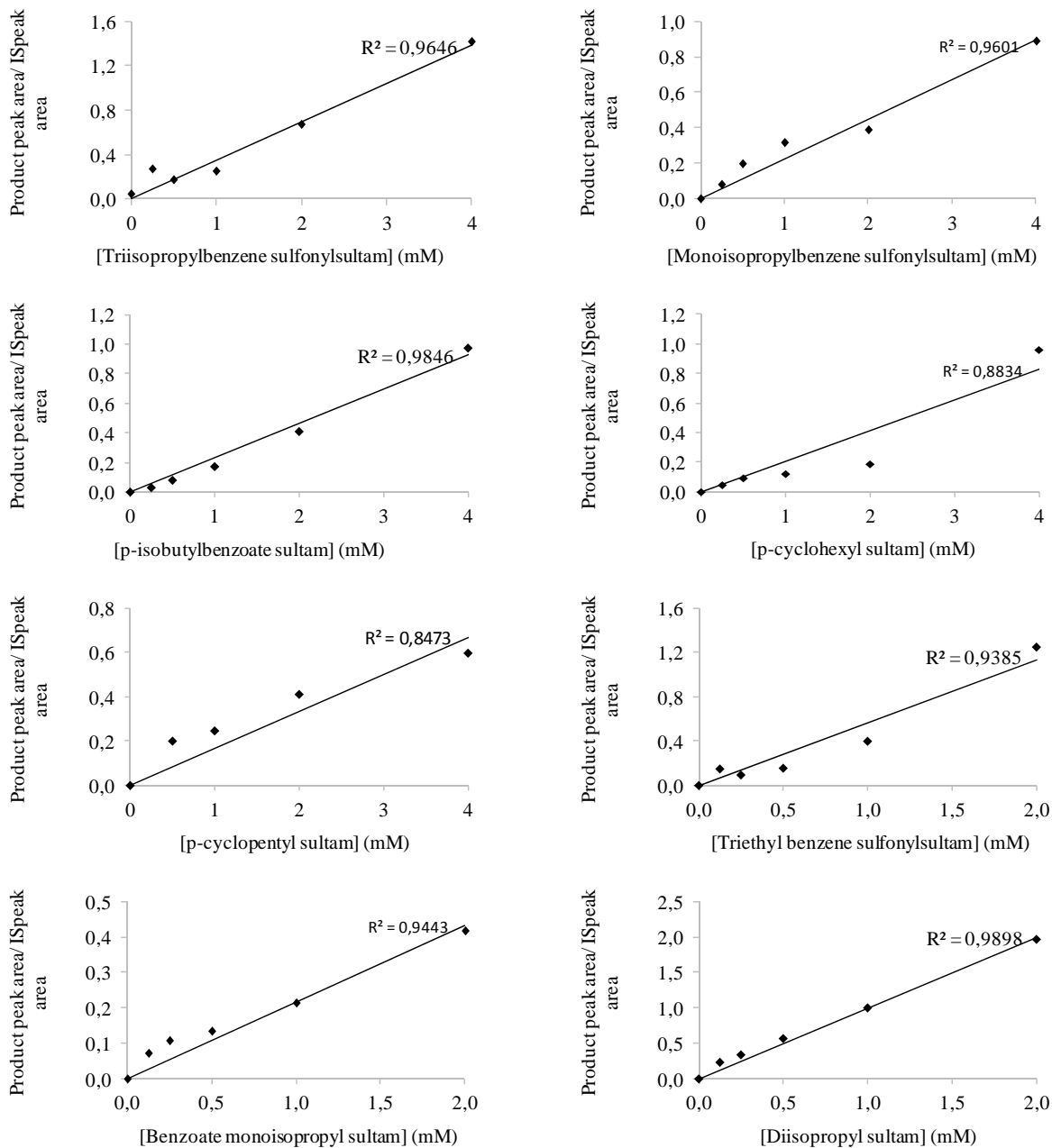
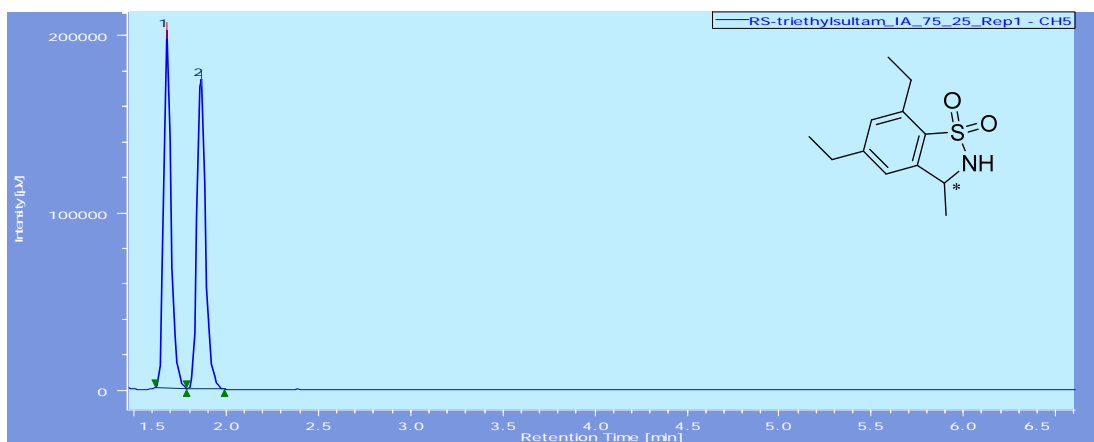


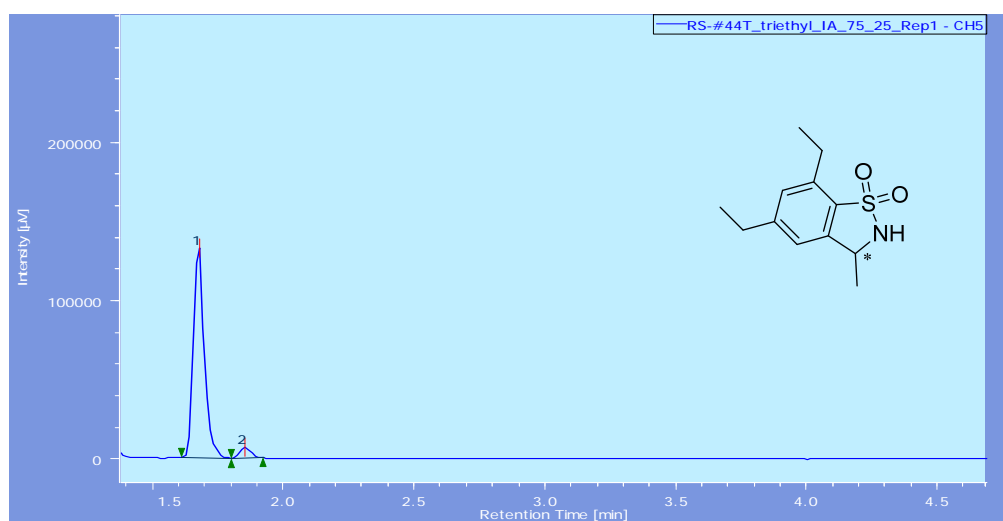
Figure S4. Representative chiral SFC chromatograms corresponding to **2b** as (a) authentic racemic standard and as produced from the reactions with (b) #139-3(T268A), (c) #J(T268A), and (d) P450_{BM3}(T268A).

(a) Racemic **2b**:



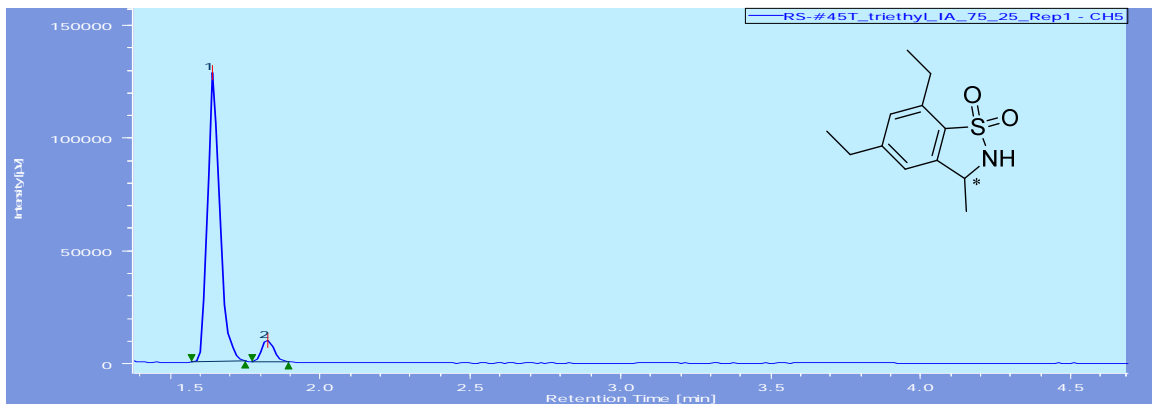
Peak Name	tR	Area%
Enantiomer 1	1.680	50.026
Enantiomer 2	1.867	49.974

(b) #139-3(T268A):



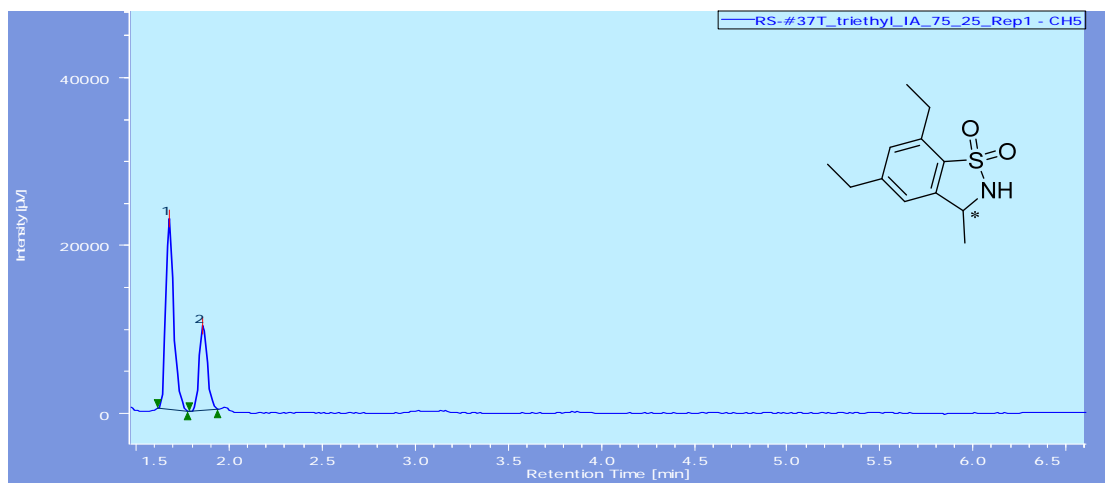
Peak Name	tR	Area%
Enantiomer 1	1.680	95.005
Enantiomer 2	1.853	4.995

(c) #J(T268A):



Peak Name	tR	Area%
Enantiomer 1	1.6400	92.837
Enantiomer 2	1.827	7.163

(d) P450_{BM3}(T268A):



Peak Name	tR	Area%
Enantiomer 1	1.680	68.611
Enantiomer 2	1.853	31.389

Table S1. Amino acid mutations in the P450_{BM3} variants investigated in this study. Amino acid residues located within the enzyme active site are underlined.

P450_{BM3} variants	Amino acid mutations compared to wild-type P450_{BM3}	Ref.
P450 _{BM3}	-	
P450 _{BM3} (T268A)	T268A	This study
139-3	<u>V78A</u> , H138Y, T175I, V178I, <u>A184V</u> , H236Q, E252G, R255S, A290V, A295T, L353V	¹
139-3(T268A)	<u>V78A</u> , H138Y, T175I, V178I, <u>A184V</u> , H236Q, E252G, R255S, <u>T268A</u> , A290V, A295T, L353V	This study
J	<u>V78A</u> , T175I, <u>A184V</u> , F205C, S226R, H236Q, E252G, R255S, A290V, L353V	²
J(T268A)	<u>V78A</u> , T175I, <u>A184V</u> , F205C, S226R, H236Q, E252G, R255S, <u>T268A</u> , A290V, L353V	This study
FL#62	<u>V78A</u> , <u>F81S</u> , <u>A82V</u> , <u>F87A</u> , P142S, T175I, <u>A180T</u> , <u>A184V</u> , A197V, F205C, S226R, H236Q, E252G, R255S, A290V, L353V	³
FL#62(T268A)	<u>V78A</u> , <u>F81S</u> , <u>A82V</u> , <u>F87A</u> , P142S, T175I, <u>A180T</u> , <u>A184V</u> , A197V, F205C, S226R, H236Q, E252G, R255S, <u>T268A</u> , A290V, L353V	This study

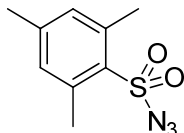
Table S2. C—H amination activity of the P450_{BM3} variants on the arylsulfonyl azide substrates **1a-3a** and **4-9**. The table reports the measured total turnover numbers for the formation of the corresponding benzosultam products **1b-9b**. (n.a. = not active).

Catalyst	Total turnovers (TTN)								
	1b	2b	3b	4b	5b	6b	7b	8b	9b
Hemin	n.a.	2	12	n.a.	n.a.	n.a.	n.a.	n.a.	n.a.
P450_{BM3}	n.a.	5	20	n.a.	18	2	n.a.	n.a.	2
P450_{BM3}(T268A)	n.a.	46	20	n.a.	1	4	49	n.a.	1
139-3	n.a.	6	16	n.a.	13	n.a.	20	n.a.	5
139-3(T268A)	n.a.	40	7	n.a.	2	3	4	n.a.	1
J	n.a.	17	51	n.a.	n.a.	3	24	n.a.	1
J(T268A)	n.a.	43	210	n.a.	5	2	44	n.a.	1
FL#62	5	47	388	5	26	13	192	1	1
FL#62(T268A)	n.a.	99	312	n.a.	3	7	21	1	1

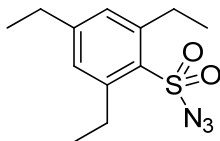
Synthetic Procedures

Chemical synthesis of arylsulfonyl azide substrates.

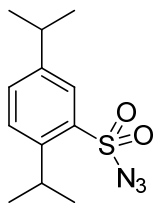
2,4,6-trimethylbenzenesulfonyl azide (**1a**), 2,4,6-triethylbenzenesulfonyl azide (**2a**), and 2,5-diisopropylsulfonyl azide (**5**), were synthesized according to reported procedures.⁴ The corresponding spectral data were found to be in agreement with the reported ones.⁴



2,4,6 trimethylbenzenesulfonyl azide (1a). ¹H NMR (400 MHz, CDCl₃): δ 7.01 (s, 2H), 2.64 (s, 6H), 2.32 (s, 3H); ¹³C NMR (100 MHz, CDCl₃): δ 144.5, 139.8, 133.0, 132.0, 22.6, 20.9; LC-MS (ESI) calculated for C₉H₁₂N₃O₂S [M+H]⁺ *m/z*: 226, Observed: 226.

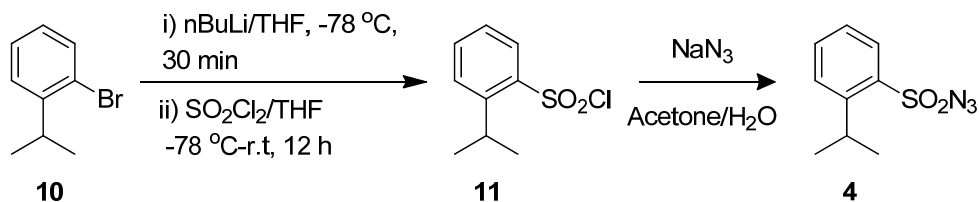


2,4,6 triethylbenzenesulfonyl azide (2a). ¹H NMR (400 MHz, CDCl₃): δ 7.08 (s, 2H), 3.06 (q, 4H, *J* = 7.3 Hz), 2.66 (q, 2H, *J* = 7.5 Hz), 1.29 (t, 6H, *J* = 7.4 Hz), 1.26 (t, 3H, *J* = 7.2 Hz); ¹³C NMR (100 MHz, CDCl₃): δ 150.7, 146.3, 132.3, 129.6, 28.5, 28.2, 16.7, 14.7; LC-MS (ESI) calculated for C₁₂H₁₈N₃O₂S [M+H]⁺ *m/z*: 268, Observed: 268.



2,5 diisopropylbenzenesulfonyl azide (5). ¹H NMR (500 MHz, CDCl₃): δ 7.89-7.87 (m, 1H), 7.54-7.50 (m, 2H), 3.70 (sep, 1H, *J* = 5.6 Hz), 2.95 (sep, 1H, *J* = 5.7 Hz), 1.30-1.25 (m, 12H); ¹³C NMR (125 MHz, CDCl₃): δ 147.1, 146.7, 135.6, 133.1, 128.5, 126.7; LC-MS (ESI) calculated for C₁₂H₁₇N₃NaO₂S [M+Na]⁺ *m/z*: 290, Observed: 290.

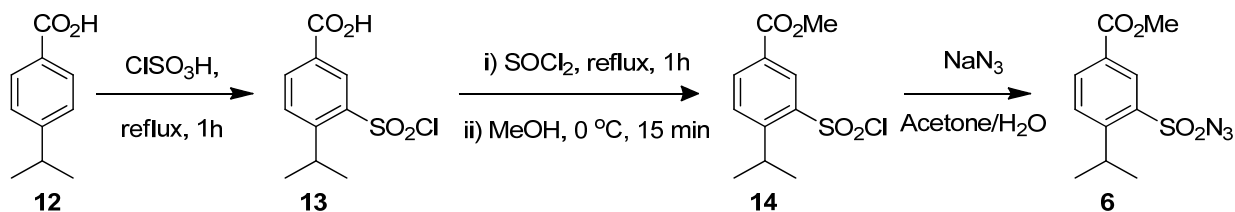
Synthesis of 2-isopropylbenzenesulfonyl azide (**4**).



To a stirred solution of 1-bromo-2-isopropylbenzene (**10**)⁵ (400 mg, 2.0 mmol) in dry THF (4.0 mL) at $-78\text{ }^\circ\text{C}$, *n*-butyl lithium (1.6 M in hexane, 0.75 mL, 2.4 mmol) was added slowly and stirred for 30 min, maintaining temperature below $-70\text{ }^\circ\text{C}$. Sulfuryl chloride (0.12 mL, 3 mmol) was then added and stirred overnight at room temperature. After the completion of reaction (as observed from TLC), reaction mixture was quenched with water followed by extraction with ether (3 x 10 mL). The combined organic layers were washed with brine, dried over Na_2SO_4 and evaporated under vacuum. Flash column chromatography of the obtained residue on a silica gel furnished 2-isopropylbenzenesulfonyl chloride (**11**) in 35% yield as a colorless oil. $R_f = 0.88$ (1% EtOAc in hexane); ^1H NMR (500 MHz, CDCl_3): δ 8.05-8.04 (m, 1H), 7.70-7.67 (m, 1H), 7.62-7.60 (m, 1H), 7.39-7.26 (m, 1H), 4.07 (sep, 1H, $J = 7.6$ Hz), 1.35 (d, 6H, $J = 7.6$ Hz); ^{13}C NMR (125 MHz, CDCl_3): δ 149.3, 142.2, 135.5, 128.9, 128.5, 126.4, 29.1, 23.7.

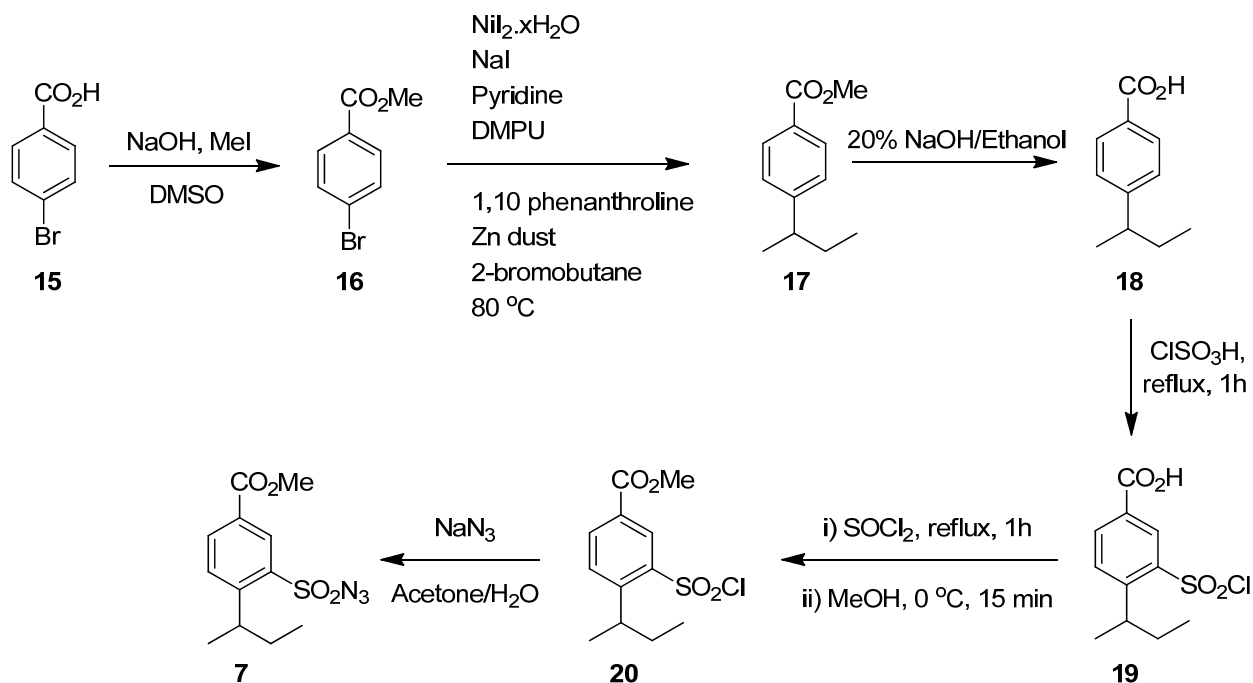
To a stirred solution of **11** (200 mg, 0.91 mmol) in acetone/water (1:1) (3 mL) at $0\text{ }^\circ\text{C}$ was added NaN_3 (89 mg, 1.3 mmol) and left stirred at room temperature. After the completion of reaction (as observed from TLC, in about 45 min), reaction mixture was concentrated under vacuum, followed by extraction with dichloromethane (3 x 10 mL). The combined organic layers were washed with brine, dried over Na_2SO_4 and evaporated under reduced pressure. The residue was purified by flash chromatography on silica gel which furnished 2-isopropylbenzenesulfonyl azide **4** as a colorless oil in 94% yield. $R_f = 0.80$ (5% EtOAc in hexane); ^1H NMR (500 MHz, CDCl_3): δ 8.04-8.02 (m, 1H), 7.67-7.64 (m, 1H), 7.59-7.58 (m, 1H), 7.40-7.35 (m, 1H), 3.74 (sep, 1H, $J = 7.5$ Hz), 1.31 (d, 6H, $J = 7.2$ Hz); ^{13}C NMR (125 MHz, CDCl_3): δ 149.7, 135.9, 134.9, 129.2, 128.6, 126.3, 29.7, 23.9. LC-MS (ESI) calculated for $\text{C}_9\text{H}_{11}\text{N}_3\text{NaO}_2\text{S}$ $[\text{M}+\text{Na}]^+$ m/z : 248, Observed: 248.

Synthesis of methyl 3-(azidosulfonyl)-4-isopropylbenzoate (**6**)



3-(chlorosulfonyl)-4-isopropylbenzoic acid (**13**) was synthesized from commercially available 4-isopropyl benzoic acid (**12**) in 65% yield following a literature procedure.⁶ $R_f = 0.35$ (5% MeOH in CHCl_3); $^1\text{H NMR}$ (400 MHz, DMSO): δ 11.2 (s, br, 1H), 8.39 (s, 1H), 7.87-7.86 (m, 1H), 7.48-7.47 (m, 1H), 4.23 (sep, 1H, $J = 6.9$ Hz), 1.19 (d, 6H, $J = 6.4$ Hz). 3-(chlorosulfonyl)-4-isopropylbenzoic acid (**13**) (0.85 mmol) was refluxed in SOCl_2 (1.0 mL) for 1h. The excess SOCl_2 was removed under reduced pressure, then methanol (3 mL) was added at 0 °C, and the solution was stirred for 15 min at room temperature. The solvent was removed under vacuum and the residue obtained was purified by flash chromatography on silica gel which furnished methyl 3-(chlorosulfonyl)-4-isopropylbenzoate (**14**) as pale yellow oil in 86% yield. $R_f = 0.75$ (10% EtOAc in Hexane); $^1\text{H NMR}$ (500 MHz, CDCl_3): δ 8.62 (s, 1H), 8.26 (d, 1H, $J = 8.3$ Hz), 7.66 (d, 1H, $J = 8.1$ Hz), 4.04 (sep, 1H, $J = 7.1$ Hz), 3.90 (s, 3H), 1.32 (d, 6H, $J = 6.8$ Hz); $^{13}\text{C NMR}$ (125 MHz, CDCl_3): δ 164.7, 154.0, 142.3, 135.9, 129.6, 129.4, 128.7, 52.6, 29.4, 23.4. Compound **14** was then converted into methyl 3-(azidosulfonyl)-4-isopropylbenzoate (**6**) in 95% yield, following a procedure identical to that described above for 2-isopropylbenzenesulfonyl azide (**4**). $R_f = 0.76$ (5% EtOAc in Hexane); $^1\text{H NMR}$ (500 MHz, CDCl_3): δ 8.64 (s, 1H), 8.26 (d, 1H, $J = 8.2$ Hz), 7.66 (d, 1H, $J = 8.1$ Hz), 3.93 (s, 3H), 3.76 (sep, 1H, $J = 6.9$ Hz), 1.30 (d, 6H, $J = 6.7$ Hz); $^{13}\text{C NMR}$ (125 MHz, CDCl_3): δ 165.0, 154.5, 136.5, 135.5, 130.3, 129.0, 128.6, 52.6, 30.1, 23.7; LC-MS (ESI) calculated for $\text{C}_{11}\text{H}_{13}\text{N}_3\text{NaO}_4\text{S}$ $[\text{M}+\text{Na}]^+$ m/z 306, Observed: 306.

Synthesis of methyl 3-(azidosulfonyl)-4-sec-butylbenzoate (**7**)

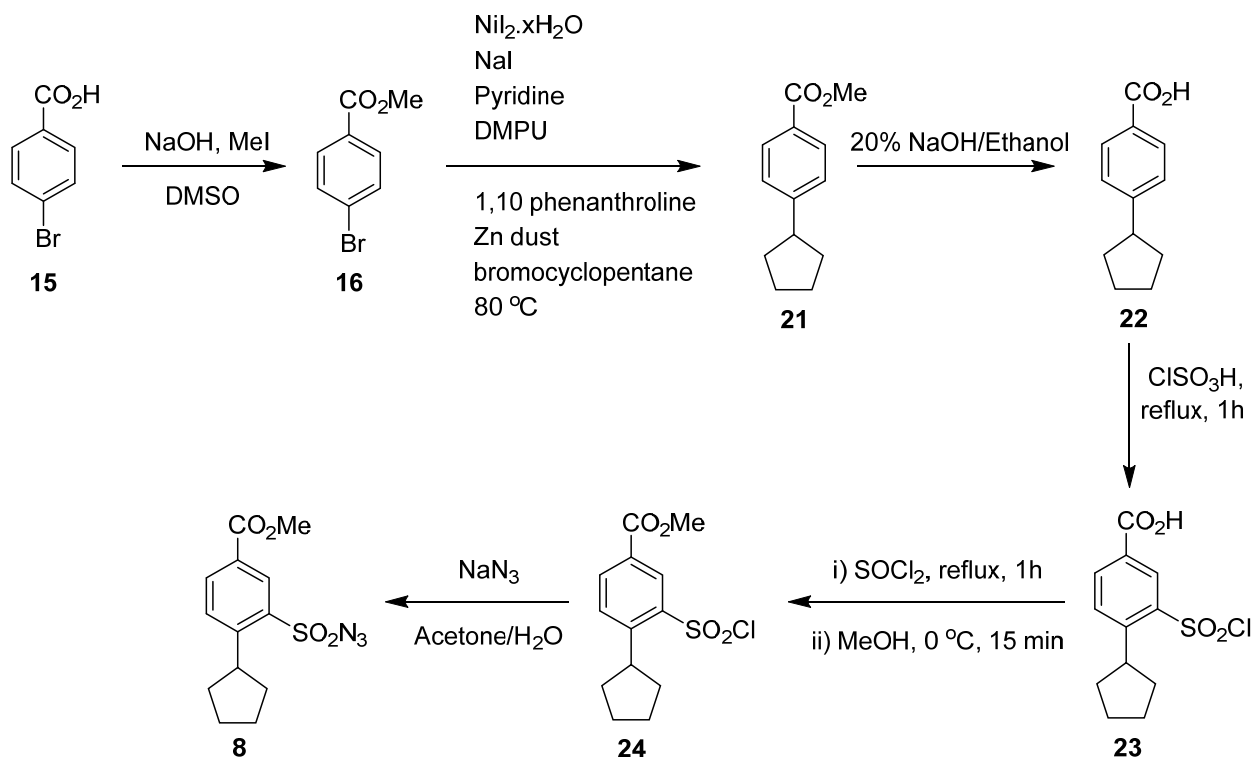


4-bromobenzoate (**16**) was synthesized starting from *p*-bromobenzoic acid (**15**) according to a previously described procedure.⁷ *p*-isobutyl methylbenzoate (**17**) was then obtained in 75% yield via nickel-catalyzed reductive coupling of 2-bromobutane with methyl 4-bromobenzoate (**16**) using a procedure reported by Weix and co-workers.⁸ $R_f = 0.82$ (5% ether in pentane); $^1\text{H NMR}$ (400 MHz, CDCl_3): δ 7.95 (d, 2H, $J = 8.3$ Hz), 7.24 (d, 2H, $J = 8.1$ Hz), 3.89 (s, 3H), 2.67-2.63 (m, 1H), 1.62-1.58 (m, 2H), 1.24 (d, 3H, $J = 7.5$ Hz), 0.82-0.79 (m, 3H); $^{13}\text{C NMR}$ (100 MHz, CDCl_3): δ 167.2, 153.8, 130.1, 127.2, 127.9, 52.1, 41.8, 30.9, 21.6, 12.1; GC-MS m/z (% relative intensity): 192(22.5), 163(100.0), 131(16.3), 91(21.6). After basic hydrolysis (20% NaOH/Ethanol) of **17** to give *p*-isobutylbenzoic acid (**18**) in quantitative yield, the latter was converted to the sulfonyl chloride **19** in 67 % yield. $R_f = 0.42$ (5% MeOH in CHCl_3); $^1\text{H NMR}$ (500 MHz, CDCl_3): δ 8.80 (s, 1H), 8.38 (d, 1H, $J = 8.2$ Hz), 7.69 (d, 1H, $J = 7.9$ Hz), 3.91-3.88 (m, 1H), 1.94-1.72 (m, 2H), 1.35 (d, 3H, $J = 7.5$ Hz), 0.93-0.92 (m, 3H); $^{13}\text{C NMR}$ (125 MHz, CDCl_3): δ 169.6, 154.5, 143.4, 136.3, 130.6, 129.7, 127.7, 36.4, 30.8, 21.7, 12.1.

Methyl 4-(sec-butyl)-3-(chlorosulfonyl)benzoate (**20**) was then synthesized in 86% yield from carboxylic acid **19** according to the procedure described above for methyl 3-(azidosulfonyl)-4-isopropylbenzoate (**6**). $R_f = 0.80$ (10% EtOAc in Hexane); $^1\text{H NMR}$ (500 MHz, CDCl_3): δ 8.70 (s, 1H), 8.30 (d, 1H, $J = 8.3$ Hz), 7.63 (d, 1H, $J = 7.9$ Hz), 3.95 (s, 3H), 3.75-3.86 (m, 1H), 1.77-1.72 (m, 2H), 1.31 (d, 3H, $J = 7.3$ Hz), 0.91-0.89 (m, 3H); $^{13}\text{C NMR}$ (125 MHz, CDCl_3): δ 164.8, 153.3, 143.1, 135.9, 129.9, 129.4, 128.7, 52.7, 36.3, 30.7, 21.7, 12.1.

Compound **20** was then converted to the desired methyl 3-(azidosulfonyl)-4-sec-butylbenzoate (**7**) in 94% yield following the procedure described above for 2-isopropylbenzenesulfonyl azide (**4**). $R_f = 0.79$ (10% EtOAc in Hexane); $^1\text{H NMR}$ (500 MHz, CDCl_3): δ 8.67 (s, 1H), 8.26 (d, 1H, $J = 7.8$ Hz), 7.60 (d, 1H, $J = 7.9$ Hz), 3.94 (s, 3H), 3.60-3.54 (m, 1H), 1.76-1.66 (m, 2H), 1.28 (d, 3H, $J = 7.1$ Hz), 0.88-0.85 (m, 3H); $^{13}\text{C NMR}$ (125 MHz, CDCl_3): δ 164.9, 153.7, 137.4, 135.3, 130.4, 129.0, 128.8, 52.4, 36.9, 30.8, 21.8, 11.8; LC-MS (ESI) calculated for $\text{C}_{11}\text{H}_{14}\text{N}_3\text{O}_4\text{S}$ $[\text{M}+\text{H}]^+$ m/z 298, Observed: 298.

Synthesis of methyl 3-(azidosulfonyl)-4-cyclopentylbenzoate (**8**)



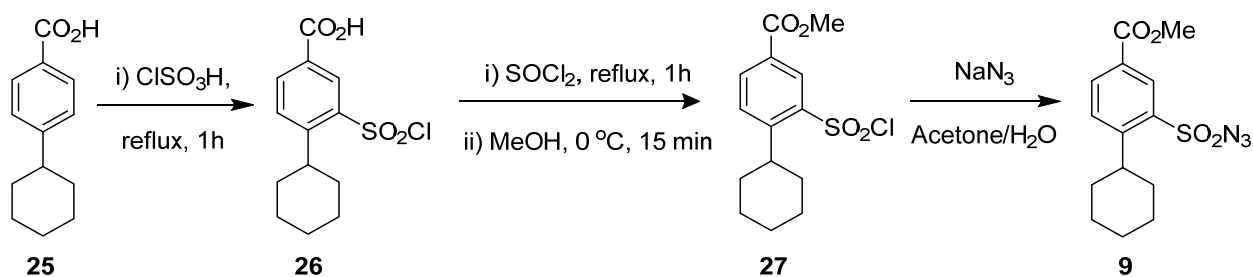
4-bromobenzoate (**16**) was synthesized starting from *p*-bromobenzoic acid (**15**) according to a previously described procedure.⁷ *p*-cyclopentyl methylbenzoate (**21**) was then obtained in 75% yield via nickel-catalyzed reductive coupling of bromocyclopentane with methyl 4-bromobenzoate (**16**) using a procedure reported by Weix and co-workers.⁸ $R_f = 0.85$ (5% ether in pentane); $^1\text{H NMR}$ (500 MHz, CDCl_3): δ 7.95 (d, 2H, $J = 8.3$ Hz), 7.28 (d, 2H, $J = 8.1$ Hz), 3.89 (s, 3H), 3.07-3.01 (m, 1H), 2.08 (m, 2H), 1.82-1.59 (m, 6H); $^{13}\text{C NMR}$ (125 MHz, CDCl_3): δ 167.2, 152.2, 129.6, 127.6, 127.1, 51.9, 45.9, 34.5, 25.6; GC-MS m/z (% relative intensity): 204(1.7), 145(6.8), 131(2.6). After basic hydrolysis (20% NaOH/Ethanol) of **21** to give *p*-4-cyclopentylbenzoic acid (**22**) in quantitative yield, the latter was converted to the sulfonyl chloride **23** in 67% yield. $R_f = 0.42$ (5% MeOH in CHCl_3); $^1\text{H NMR}$ (500 MHz, CDCl_3): δ 8.80 (s, 1H), 8.36 (d, 1H, $J = 8.2$ Hz), 7.69 (d, 1H, $J = 8.1$ Hz), 4.15-4.11 (m, 1H), 2.25 (m, 2H), 1.87-1.61 (m, 6H); $^{13}\text{C NMR}$ (125 MHz, CDCl_3): δ 169.3, 154.3, 143.4, 136.2, 130.4, 130.3, 127.5, 41.2, 36.2, 26.5.

Methyl 3-(chlorosulfonyl)-4-cyclopentylbenzoate (**24**) was synthesized in 81% yield from carboxylic acid **23** according to the procedure described above for methyl 3-(azidosulfonyl)-4-isopropylbenzoate (**6**). $R_f = 0.79$ (10% EtOAc in Hexane); $^1\text{H NMR}$ (500 MHz, CDCl_3): δ 8.65 (s, 1H), 8.27 (d, 1H, $J = 8.3$ Hz), 7.66

(d, 1H, $J = 8.0$ Hz), 4.07-4.02 (m, 1H), 3.94 (s, 3H), 2.26-2.25 (m, 2H), 1.90-1.63 (m, 6H); ^{13}C NMR (125 MHz, CDCl_3): δ 164.8, 153.1, 143.1, 135.8, 130.1, 129.6, 128.5, 52.6, 41.1, 36.1, 26.4.

Compound **24** was converted to methyl 3-(azidosulfonyl)-4-cyclopentylbenzoate (**8**) in 95% yield following procedure as described for 2-isopropylbenzenesulfonyl azide (**4**). $R_f = 0.79$ (10% EtOAc in Hexane); ^1H NMR (500 MHz, CDCl_3): δ 8.64 (s, 1H), 8.25 (d, 1H, $J = 8.2$ Hz), 7.64 (d, 1H, $J = 8.1$ Hz), 3.94 (s, 3H), 3.77-3.73 (m, 1H), 2.19 (m, 2H), 1.88-1.61(m, 6H); ^{13}C NMR (125 MHz, CDCl_3): δ 165.1, 153.4, 137.3, 135.4, 130.2, 129.7, 128.3, 52.6, 41.6, 36.2, 26.3; LC-MS (ESI) calculated for $\text{C}_{13}\text{H}_{16}\text{N}_3\text{O}_4\text{S}$ $[\text{M}+\text{H}]^+$ m/z : 310, Observed 310.

Synthesis of methyl 3-(azidosulfonyl)-4-cyclohexylbenzoate (**9**)

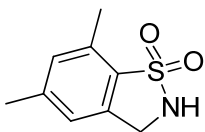


3-(chlorosulfonyl)-4-cyclohexylbenzoic acid (**26**) was synthesized from commercially available 4-cyclohexyl benzoic acid (**25**) in 64% yield following a literature procedure.⁸ $R_f = 0.37$ (5% MeOH in CHCl_3); ^1H NMR (400 MHz, DMSO): δ 13.2 (s, br, 1H), 8.33 (s, 1H), 7.80-7.78 (m, 1H), 7.39-7.38 (m, 1H), 3.83 (m, 1H), 1.74 (m, 5H), 1.31-1.22 (m, 5H).

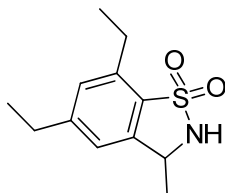
Methyl 3-(chlorosulfonyl)-4-cyclohexylbenzoate (**27**) was obtained in 82% yield from carboxylic acid **26** as pale yellow oil following a procedure identical to that described above for methyl 3-(chlorosulfonyl)-4-isopropylbenzoate (**14**). $R_f = 0.77$ (10% EtOAc in Hexane); ^1H NMR (500 MHz, CDCl_3): δ 8.70 (s, 1H), 8.30 (d, 1H, $J = 8.2$ Hz), 7.67 (d, 1H, $J = 8.1$ Hz), 3.96 (s, 3H), 3.71 (m, 1H), 1.97-1.82 (m, 5H), 1.50-1.26 (m, 5H); ^{13}C NMR (125 MHz, CDCl_3): δ 164.9, 152.8, 142.6, 135.8, 130.0, 129.8, 128.6, 52.7, 40.1, 33.8, 26.4, 25.9. Compound **27** was then converted into methyl 3-(azidosulfonyl)-4-cyclohexylbenzoate (**9**) in 94% yield, following a procedure identical to that described above for 2-isopropylbenzenesulfonyl azide (**4**). $R_f = 0.76$ (10% EtOAc in Hexane); ^1H NMR (500 MHz, CDCl_3): δ 8.67 (s, 1H), 8.26 (d, 1H, $J = 8.2$ Hz), 7.64 (d, 1H, $J = 7.9$ Hz), 3.95 (s, 3H), 3.36 (m, 1H), 1.87-1.78 (m, 5H), 1.50-1.24 (m, 5H); ^{13}C NMR (125 MHz, CDCl_3): δ 165.1, 153.3, 136.7, 135.3, 130.4, 129.7, 128.5, 52.6, 40.7, 34.1, 26.5, 25.8; LC-MS (ESI) calculated for $\text{C}_{14}\text{H}_{17}\text{N}_3\text{NaO}_4\text{S}$ $[\text{M}+\text{Na}]^+$ m/z : 346, Observed: 346.

Chemical synthesis of benzosultam standards

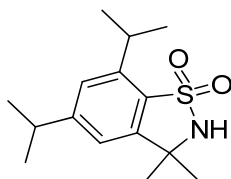
To generate authentic standards for the P450-catalyzed C—H amination reactions, benzosultams **1b-9b** were prepared from the respective arylsulfonyl azide substrates using Co-(TPP) catalyst according to previously reported procedures.⁴ Briefly, in an oven-dried Schlenk tube, strictly following Schlenk technique, benzenesulfonyl azide (0.2 mmol), catalyst Co-(TPP) (0.004 mmol), and 5Å MS (100 mg) were mixed in toluene (2 mL). After 12-18 hours, the crude products were purified by flash chromatography (25-35% EtOAc in hexane) to give benzosultams **1b-9b**.



5,7-dimethyl-2,3-dihydrobenzo[d]isothiazole 1,1-dioxide (1b). ¹H NMR (500 MHz, CDCl₃): δ 7.06 (s, 1H), 6.96 (s, 1H), 4.64 (s, 1H), 4.43 (d, 2H, *J* = 5.8 Hz), 2.59 (s, 3H), 2.39 (s, 3H); ¹³C NMR (125 MHz, CDCl₃): δ 144.2, 137.2, 134.1, 131.6, 131.4, 122.2, 45.1, 21.5, 16.9; GC-MS *m/z* (% relative intensity): 197(100.0), 132(89.2), 182(18.0).

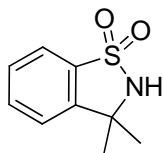


(±)-5,7-diethyl-3-methyl-2,3-dihydrobenzo[d]isothiazole 1,1-dioxide (2b). ¹H NMR (400 MHz, CDCl₃): δ 7.10 (s, 1H), 6.97 (s, 1H), 4.98 (s, 1H), 4.69-4.64 (m, 1H), 2.98 (q, 2H, *J* = 7.6 Hz), 2.71 (q, 2H, *J* = 7.4 Hz), 1.55 (d, 3H, *J* = 6.9 Hz), 1.32 (t, 3H, *J* = 7.4 Hz), 1.23 (t, 3H, *J* = 7.6 Hz). ¹³C NMR (125 MHz, CDCl₃): δ 150.6, 142.5, 140.1, 131.2, 128.6, 120.3, 52.6, 28.9, 24.2, 21.5, 15.3, 14.6; GC-MS *m/z* (% relative intensity): 239(8.6), 224(100.0), 160(8.5), 144(7.6), 210(4.3).

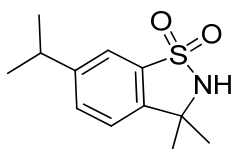


5,7-diisopropyl-3,3-dimethyl-2,3-dihydrobenzo[d]isothiazole 1,1-dioxide (3b). ¹H NMR (500 MHz, CDCl₃): δ 7.21 (s, 1H), 6.98 (s, 1H), 4.42 (s, 1H), 3.60 (sep, 1H, *J* = 6.7 Hz), 2.97 (sep, 1H, *J* = 6.7 Hz), 6.2 (s, 6H), 1.34 (d, 6H, *J* = 6.8 Hz), 1.27 (d, 6H, *J* = 6.8 Hz); ¹³C NMR (125 MHz, CDCl₃): δ 155.6,

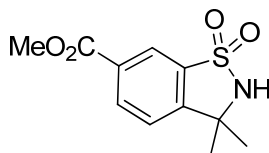
146.7, 145.3, 131.2, 124.4, 117.7, 59.7, 34.6, 29.9, 29.4, 23.9, 23.6; GC-MS m/z (% relative intensity): 182(1.8), 266(100.0), 267(16.7), 268(6.1), 250(1.4), 172(3.4).



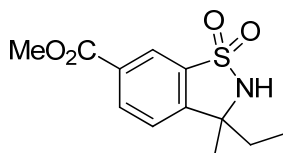
3,3-dimethyl-2,3-dihydrobenzo[d]isothiazole 1,1-dioxide (4b). ^1H NMR (500 MHz, CDCl_3): δ 7.74-7.73 (m, 1H), 7.64-7.61 (m, 1H), 7.52-7.49 (m, 1H), 7.40-7.38 (m, 1H), 4.66 (s, 1H), 1.66 (s, 6H); ^{13}C NMR (125 MHz, CDCl_3): δ 146.1, 135.2, 133.4, 129.1, 122.8, 121.2, 60.9, 29.7; GC-MS m/z (% relative intensity): 198(1.1), 182(100.0), 117(11.0).



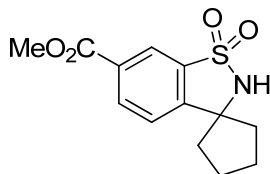
6-isopropyl-3,3-dimethyl-2,3-dihydrobenzo[d]isothiazole 1,1-dioxide (5b). ^1H NMR (500 MHz, CDCl_3): δ 7.57 (s, 1H), 7.48 (dd, 1H, $J_1 = 8.0$ Hz, $J_2 = 2.0$ Hz), 7.28 (d, 1H, $J = 7.9$ Hz), 4.70 (s, 1H), 3.01 (sep, 1H, $J = 7.1$ Hz), 1.63 (s, 6H), 1.27 (d, 6H, $J = 7.1$ Hz); ^{13}C NMR (125 MHz, CDCl_3): δ 150.6, 143.5, 135.1, 132.1, 122.6, 118.5, 60.6, 33.9, 29.7, 23.7; GC-MS m/z (% relative intensity): 224(100.0), 196(3.3), 182(7.4), 144(17.1), 130(16.8).



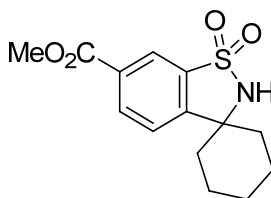
Methyl 3,3-dimethyl-2,3-dihydrobenzo[d]isothiazole-6-carboxylate 1,1-dioxide (6b). ^1H NMR (500 MHz, CDCl_3): δ 8.37 (s, 1H), 8.27 (d, 1H, $J = 8.2$ Hz), 7.46 (d, 1H, $J = 8.1$ Hz), 4.97 (s, 1H), 3.95 (s, 3H), 1.67 (s, 6H); ^{13}C NMR (125 MHz, CDCl_3): δ 165.1, 150.5, 135.9, 134.5, 131.5, 123.1, 122.9, 60.9, 52.7, 29.4; GC-MS m/z (% relative intensity): 255(2.9), 240(100.0), 241(12.2), 224(5.0), 181(7.0).



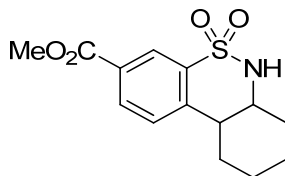
(±)-Methyl 3-ethyl-3-methyl-2,3-dihydrobenzo[d]isothiazole-6-carboxylate 1,1-dioxide (**7b**). Yield = 96%; $R_f = 0.42$ (30% EtOAc in Hexane); $^1\text{H NMR}$ (500 MHz, CDCl_3): δ 8.36 (s, 1H), 8.27 (d, 1H, $J = 8.2$ Hz), 7.42 (d, 1H, $J = 8.1$ Hz), 5.08 (s, 1H), 3.96 (s, 3H), 1.93-1.91 (m, 2H), 1.62 (d, 3H, $J = 7.3$ Hz), 0.88-0.85 (m, 3H); $^{13}\text{C NMR}$ (125 MHz, CDCl_3): δ 165.1, 149.1, 136.1, 134.3, 131.5, 123.3, 123.0, 64.5, 52.7, 34.5, 27.6, 8.4; GC-MS m/z (% relative intensity): 270(1.1), 254(6.0), 240(100.0), 238(2.9).



methyl 2H-spiro[benzo[d]isothiazole-3,1'-cyclopentane]-6-carboxylate 1,1-dioxide (**8b**). $^1\text{H NMR}$ (500 MHz, CDCl_3): δ 8.34 (s, 1H), 8.26 (d, 1H, $J = 8.3$ Hz), 7.44 (d, 1H, $J = 8.1$ Hz), 4.88 (s, 1H), 3.95 (s, 3H), 2.17-2.11 (m, 2H), 2.11-2.05 (m, 2H), 1.98 (m, 4H); $^{13}\text{C NMR}$ (125 MHz, CDCl_3): δ 165.1, 149.8, 137.1, 134.3, 131.3, 123.1, 122.6, 71.1, 52.7, 41.6, 24.7; GC-MS m/z (% relative intensity): 281(21.0), 252 (100.0), 266 (8.8), 216(22), 217(25), 202(17.4).



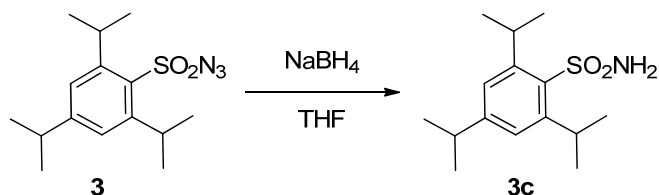
methyl 2H-spiro[benzo[d]isothiazole-3,1'-cyclohexane]-6-carboxylate 1,1-dioxide (**9b**). $^1\text{H NMR}$ (500 MHz, CDCl_3): δ 8.35 (s, 1H), 8.25 (d, 1H, $J = 8.2$ Hz), 7.46 (d, 1H, $J = 8.1$ Hz), 5.12 (s, 1H), 3.94 (s, 3H), 1.87-1.81 (m, 7H), 1.64-1.61 (m, 2H), 1.35-1.32 (m, 1H); $^{13}\text{C NMR}$ (125 MHz, CDCl_3): δ 165.1, 150.6, 136.2, 134.3, 131.5, 123.4, 122.9, 63.9, 52.7, 37.4, 24.7, 22.3; GC-MS m/z (% relative intensity): 295(16.7), 252 (100.0), 231(49.5), 230(26.4), 216(41.5).



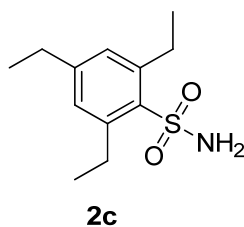
methyl 6a,7,8,9,10,10a-hexahydro-6H-dibenzo[c,e][1,2]thiazine-3-carboxylate 5,5-dioxide (**9bb**). $^1\text{H NMR}$ (500 MHz, CDCl_3): δ 8.46 (s, 1H), 8.11 (d, 1H, $J = 8.2$ Hz), 7.48 (d, 1H, $J = 8.1$ Hz), 4.54 (d, 1H, $J = 14.6$ Hz), 3.93 (s, 3H), 3.57-3.46 (m, 1H), 2.75-2.69 (m, 1H), 2.55-2.52 (m, 1H), 2.17-2.14 (m, 1H),

1.94 (m, 2H), 1.51-1.20 (m, 4H); ^{13}C NMR (125 MHz, CDCl_3): δ 165.3, 143.3, 138.4, 132.8, 129.4, 126.6, 125.7, 57.5, 52.5, 42.7, 33.5, 29.2, 25.6, 25.0; GC-MS m/z (% relative intensity): 295(100.0), 264(8.9), 252(38.2), 231(11.1), 216(13.2), 188(25.8). This product was formed in minor amount along with the five-membered major product **9b**.

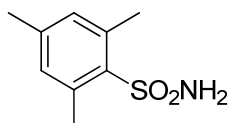
General procedure for the synthesis of representative arylsulfonamide standards



To a stirred solution of 2,4,6-triisopropylbenzenesulfonyl azide (**3a**) (0.161 mmol) in anhydrous THF (2 mL) at 0 °C was added sodium borohydride (0.162 mmol). After the completion of reaction (30 min) as observed from TLC, the reaction mixture was poured into a 10% HCl solution, and extracted with diethylether (10 x 3 mL). The combined organic layers were then washed with brine, dried over Na_2SO_4 and concentrated under vacuum. Flash column chromatography of the obtained residue on silica gel furnished 2,4,6-triisopropylbenzenesulfonamide (**3c**) as white solid in 86% yield. $R_f = 0.56$ (35% EtOAc in hexane); ^1H NMR (500 MHz, CDCl_3): δ 7.17-7.16 (m, 2H), 5.03 (s, 1H), 4.11 (sep, 2H, $J = 5.3$ Hz), 2.90 (sep, 1H, $J = 5.5$ Hz), 1.29-1.24 (m, 18H); ^{13}C NMR (125 MHz, CDCl_3): δ 152.7, 149.1, 134.9, 123.6, 34.2, 29.8, 24.7, 23.6; LC-MS(APCI) m/z : 282 $[\text{M}-\text{H}]^+$, 267 $[\text{M}-\text{CH}_4]^+$.



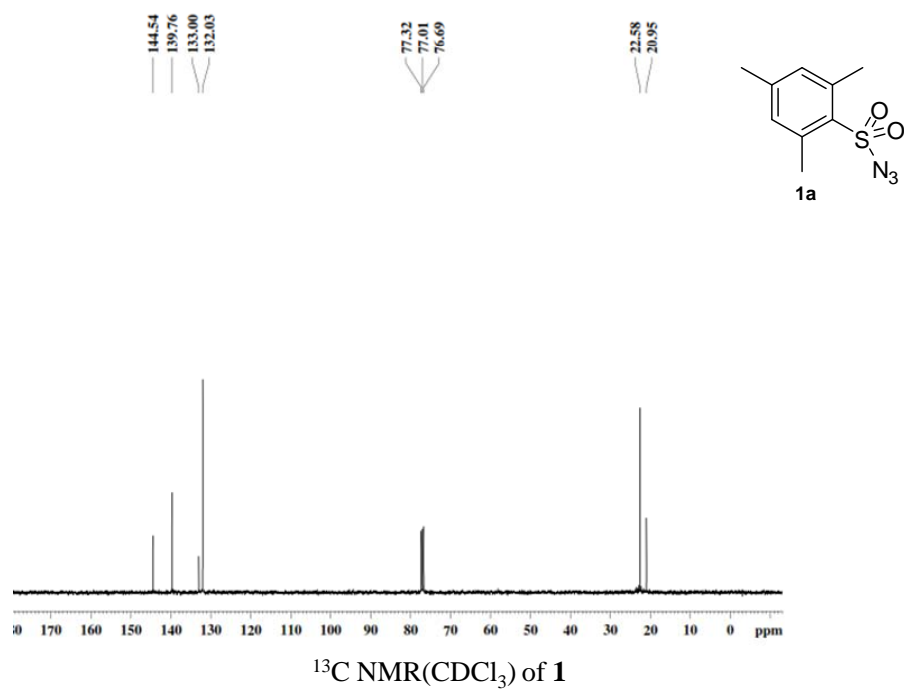
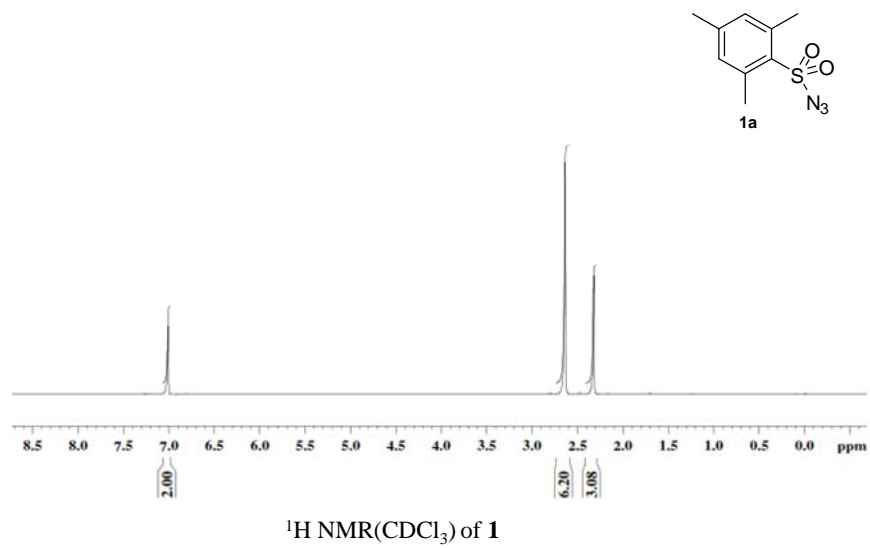
2,4,6-triethylbenzenesulfonamide (2c). Following the same procedure described above for **3a**, 2,4,6-triethylbenzenesulfonyl azide (**2a**) (0.187 mmol), NaBH_4 (0.188 mmol), in THF (2 mL) furnished compound **2c** as white solid in 88% yield. $R_f = 0.57$ (35% EtOAc in hexane); ^1H NMR (400 MHz, CDCl_3): δ 7.00 (s, 2H), 5.03 (s, 2H), 3.05 (q, 4H, $J = 7.4$ Hz), 2.60 (q, 2H, $J = 7.4$ Hz), 1.27 (t, 6H, $J = 7.3$ Hz), 1.23 (t, 3H, $J = 7.6$ Hz); ^{13}C NMR (100 MHz, CDCl_3): δ 148.4, 144.5, 135.4, 129.2, 28.4, 28.3, 16.6, 14.9; LC-MS(APCI) m/z : 240 $[\text{M}-\text{H}]^+$.

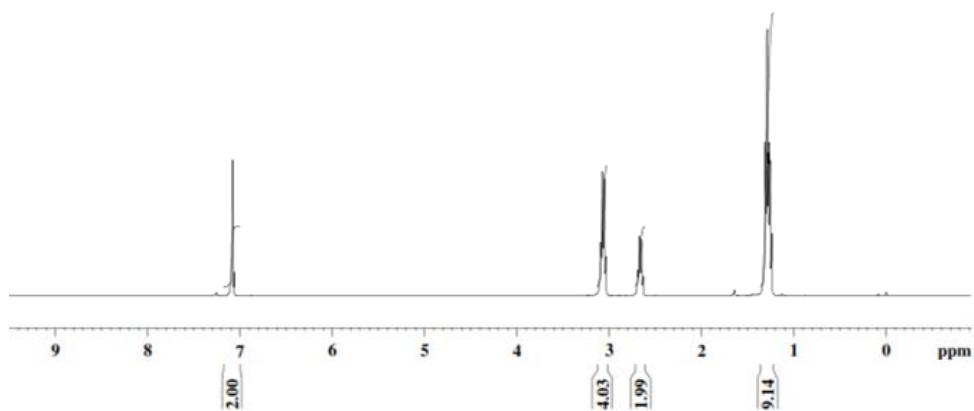
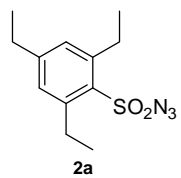


1c

2,4,6-trimethylbenzenesulfonamide (1c). Following similar procedure as described for **3a**, 2,4,6-trimethylbenzenesulfonyl azide (**1a**) (0.187 mmol), NaBH₄ (0.188 mmol), in THF (2 mL) furnished compound **1c** as white solid in 85% yield. R_f = 0.52 (35% EtOAc in hexane); ¹H NMR (400 MHz, CDCl₃): δ 6.96 (s, 2H), 4.79 (s, 2H), 2.65 (s, 6H), 2.30 (s, 3H); ¹³C NMR (100 MHz, CDCl₃): δ 142.2, 138.2, 135.9, 131.9, 22.9, 20.9; LC-MS(APCI) m/z: 98[M-H]⁺.

Spectral Data



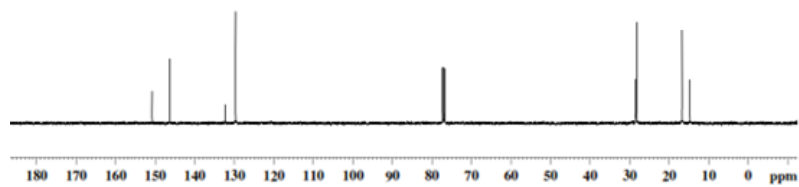
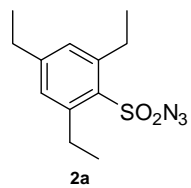


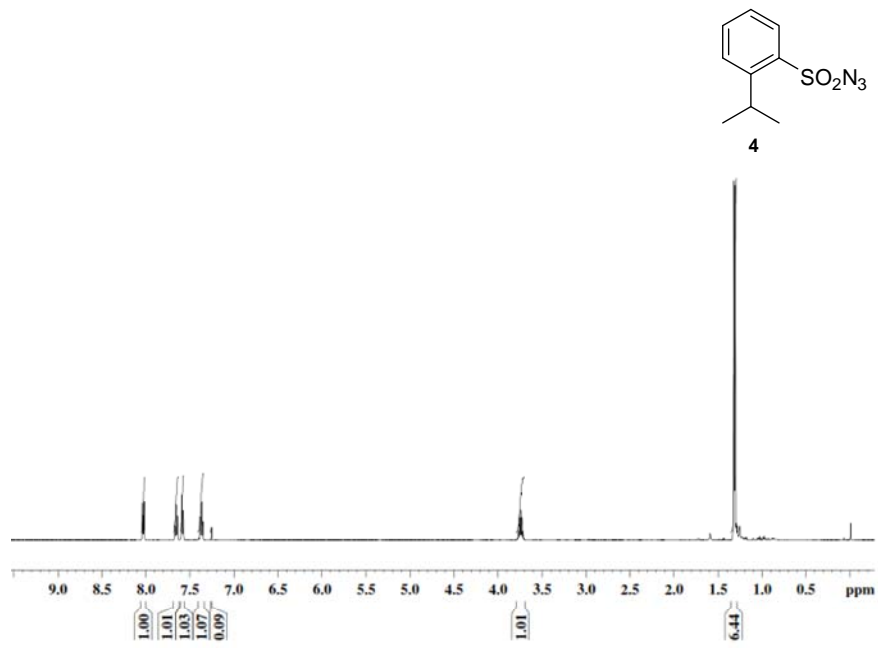
150.70
146.30

133.29
129.61

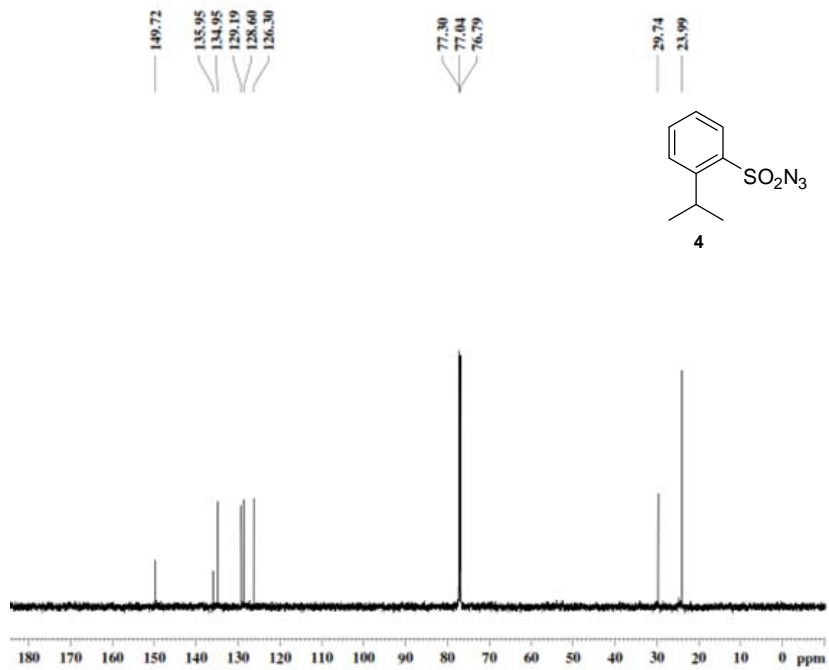
77.32
77.01
76.69

28.49
28.35
16.75
14.74

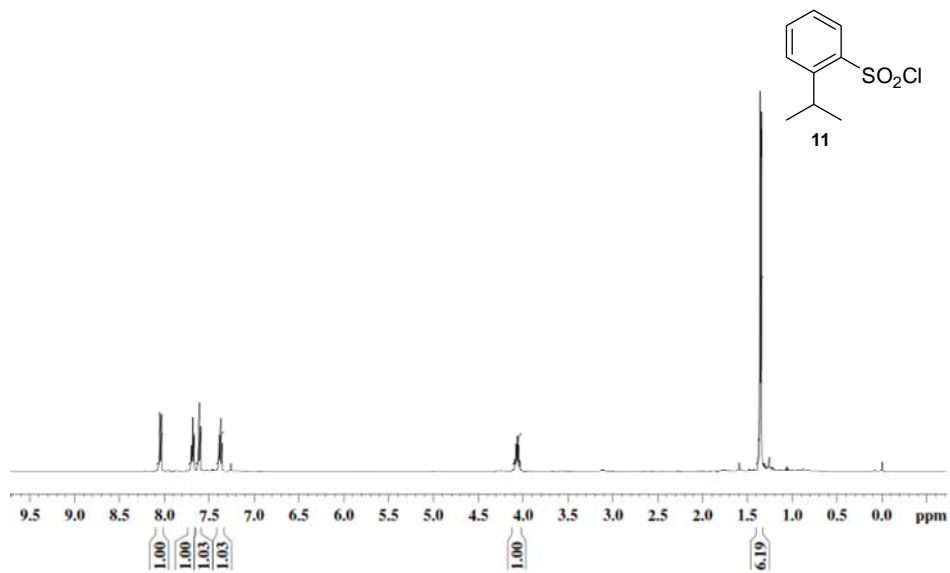




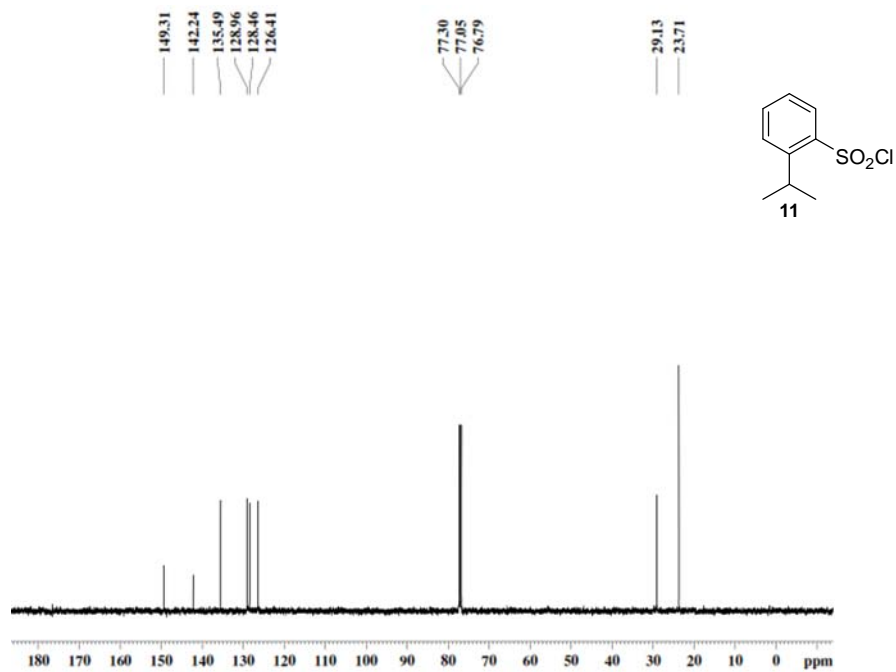
$^1\text{H NMR}(\text{CDCl}_3)$ of **4**



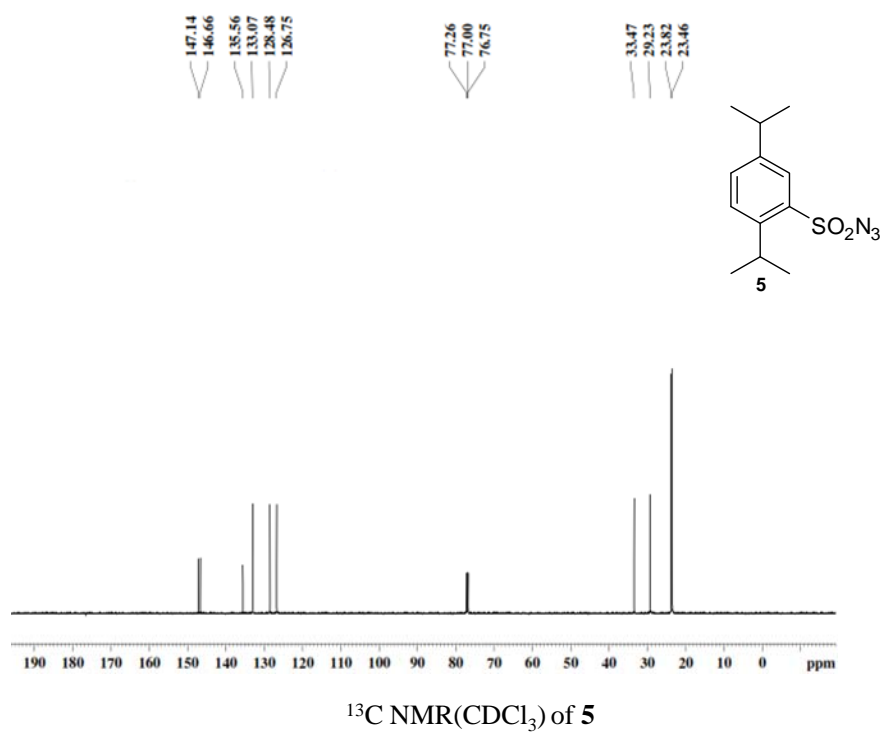
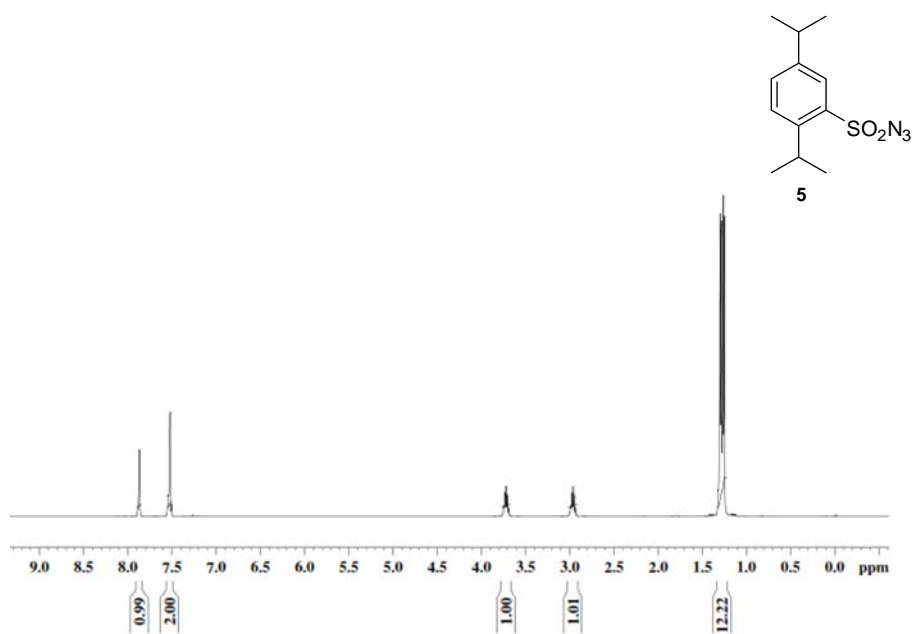
$^{13}\text{C NMR}(\text{CDCl}_3)$ of **4**

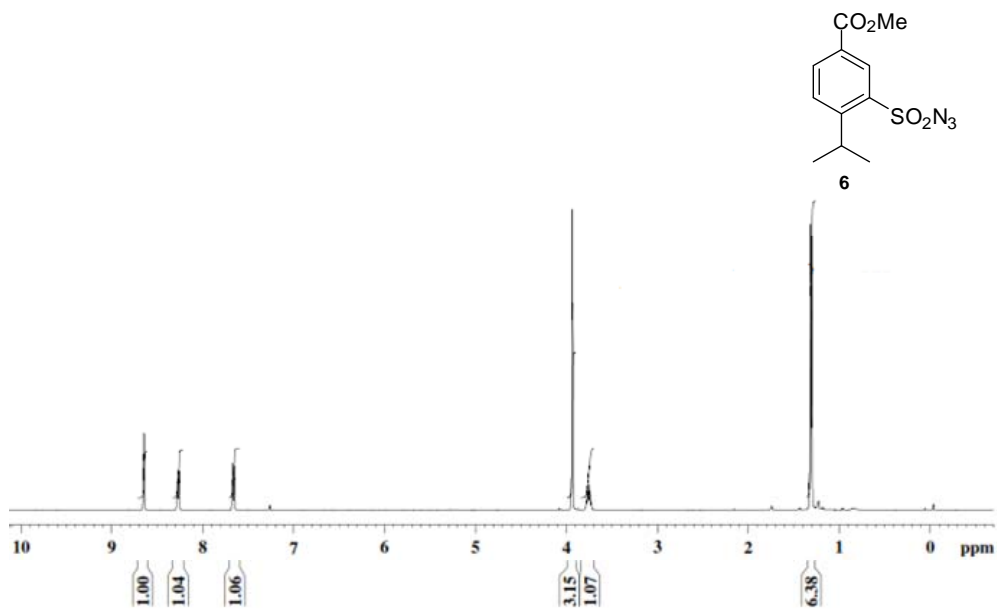


$^1\text{H NMR}(\text{CDCl}_3)$ of **11**

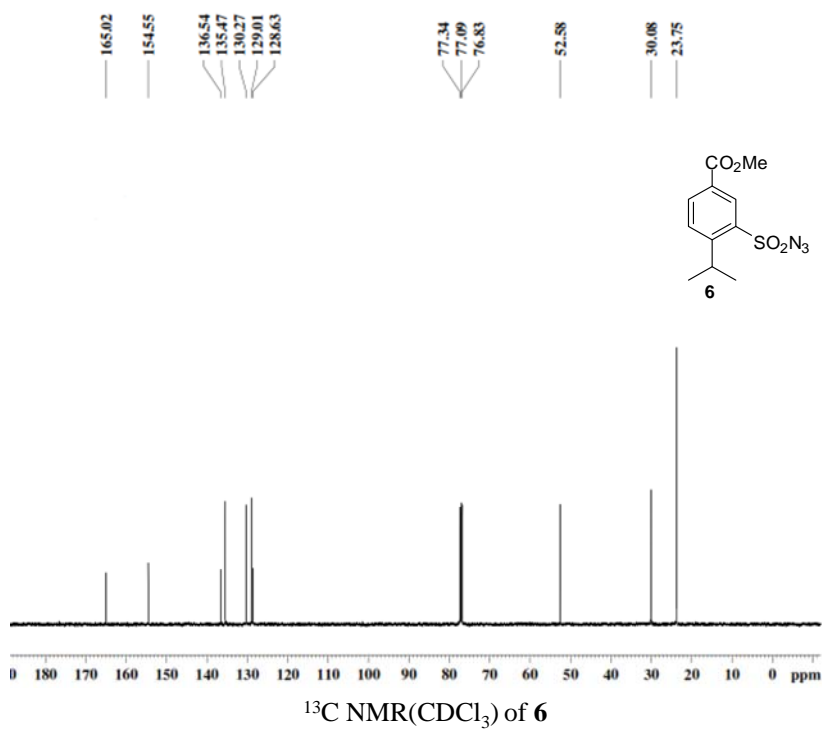


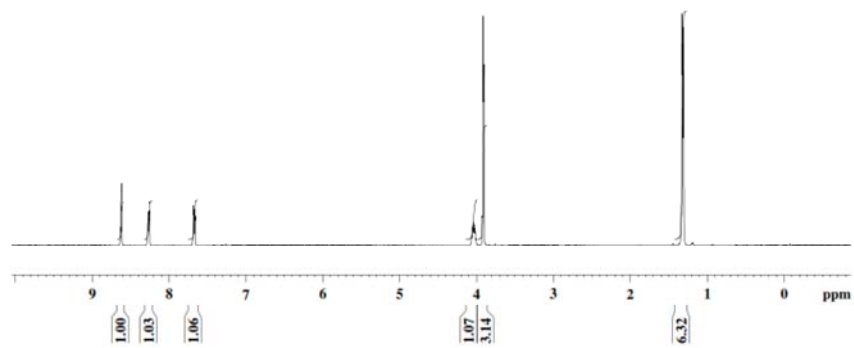
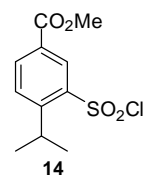
$^{13}\text{C NMR}(\text{CDCl}_3)$ of **11**



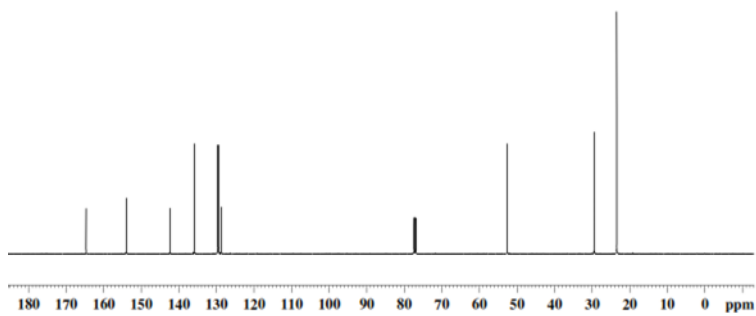
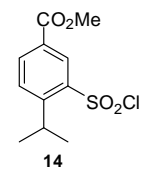


$^1\text{H NMR}(\text{CDCl}_3)$ of **6**

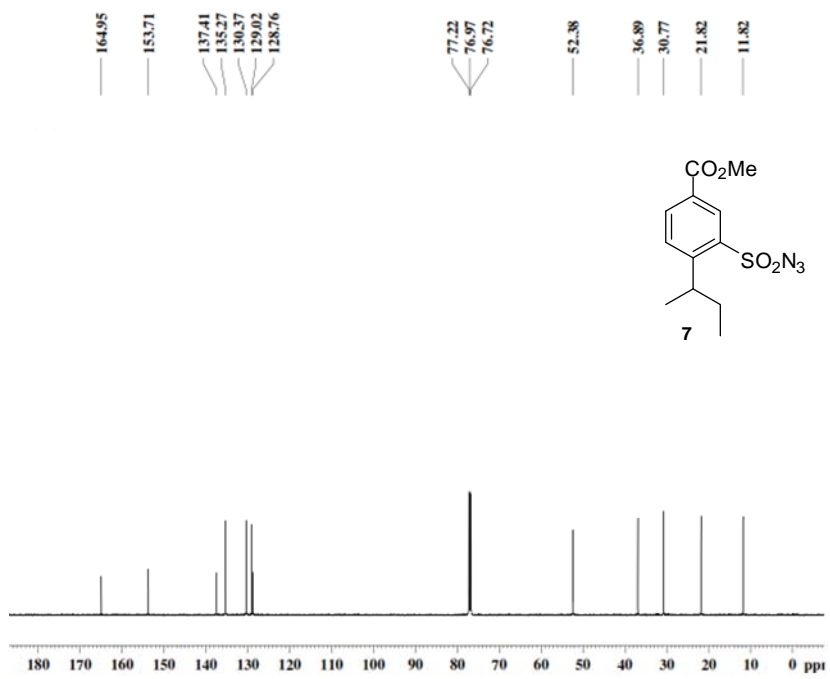
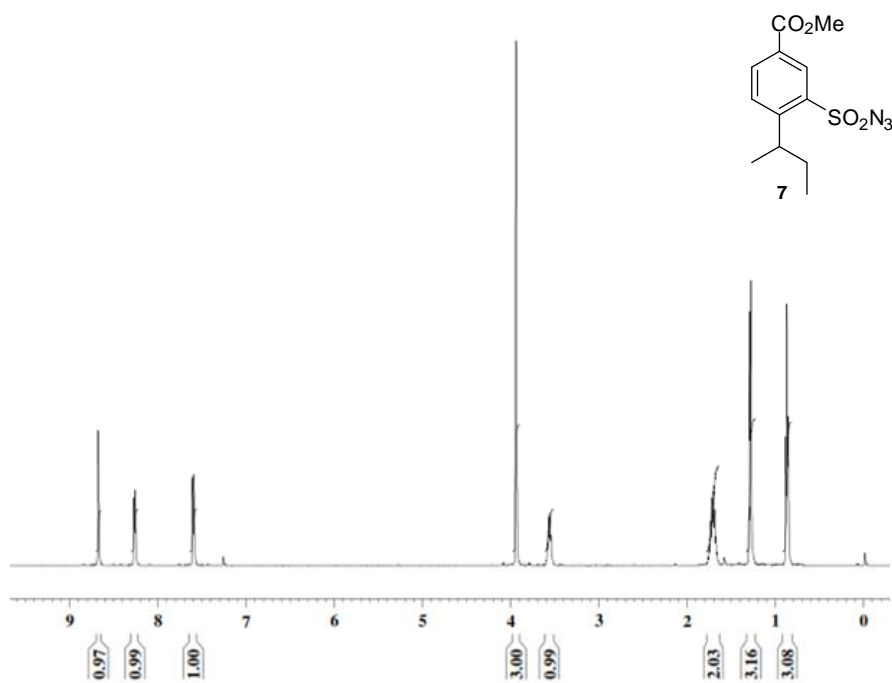


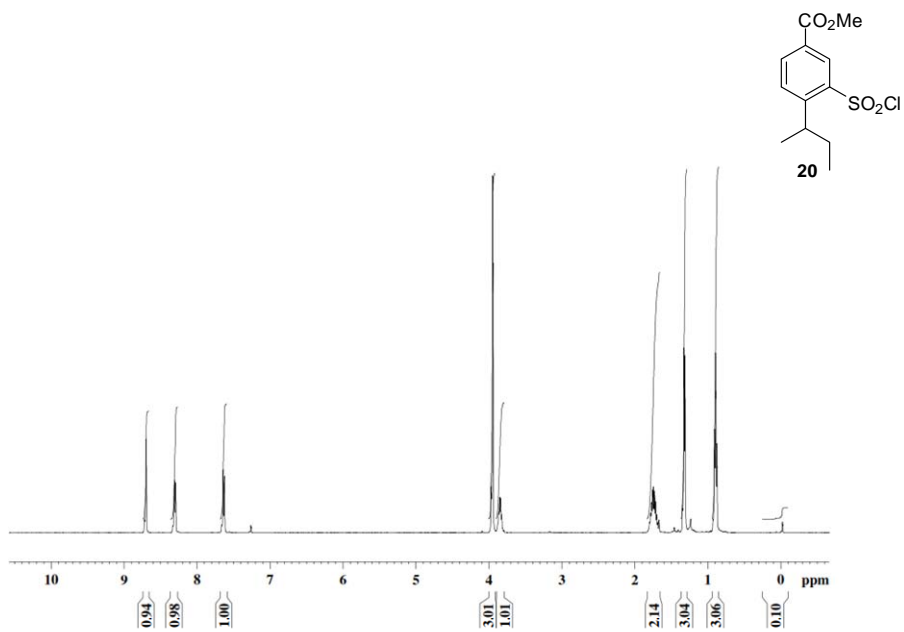


$^1\text{H NMR}(\text{CDCl}_3)$ of **14**

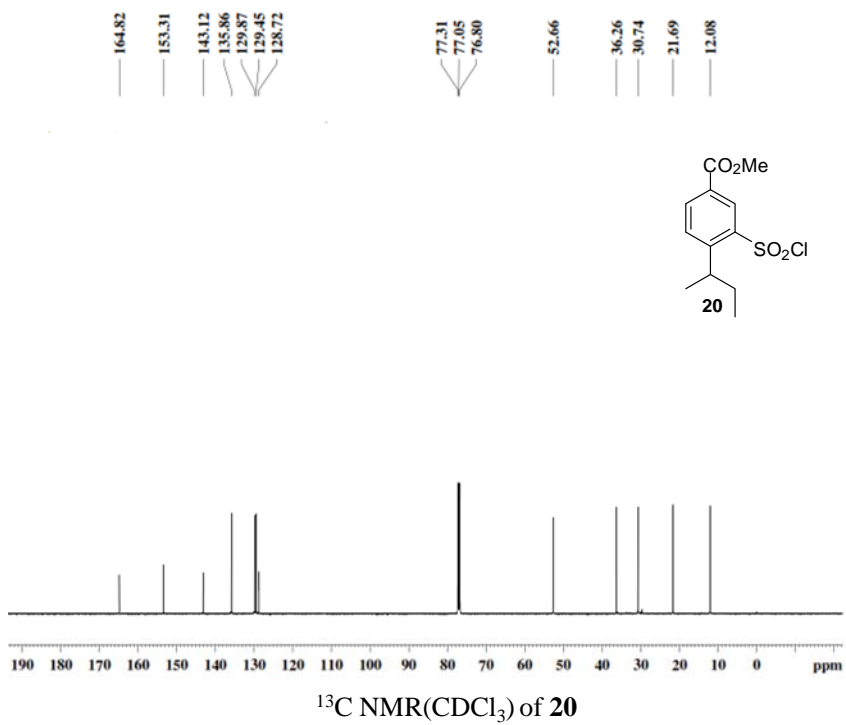


$^{13}\text{C NMR}(\text{CDCl}_3)$ of **14**

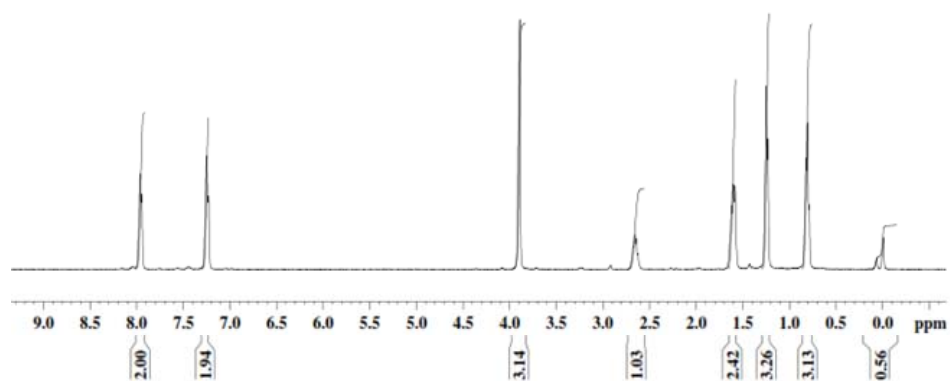
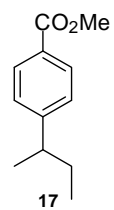




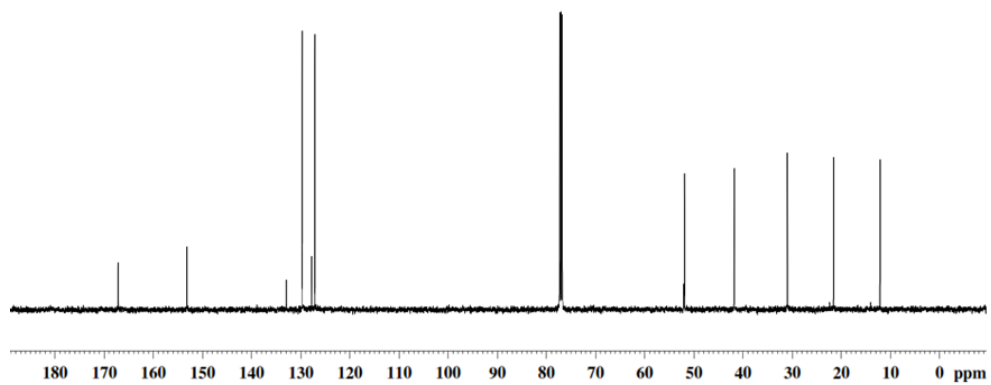
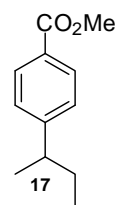
$^1\text{H NMR}(\text{CDCl}_3)$ of **20**



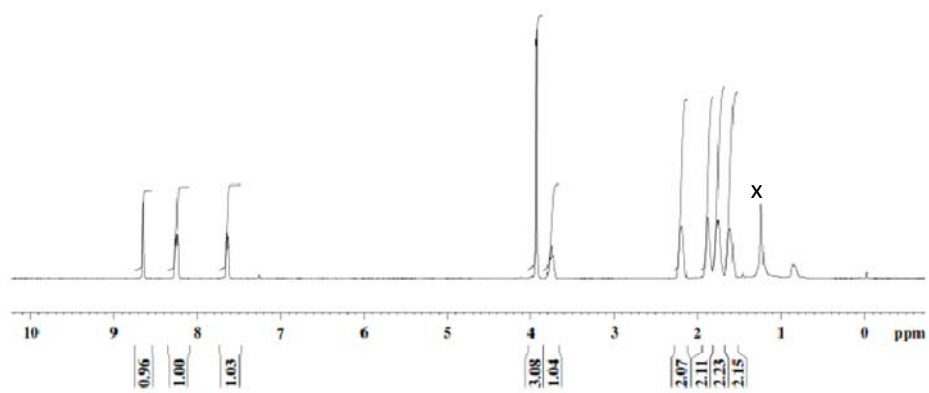
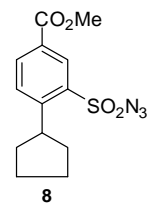
$^{13}\text{C NMR}(\text{CDCl}_3)$ of **20**



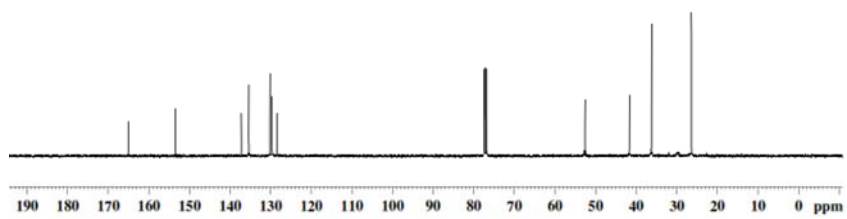
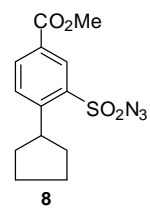
$^1\text{H NMR}(\text{CDCl}_3)$ of **17**



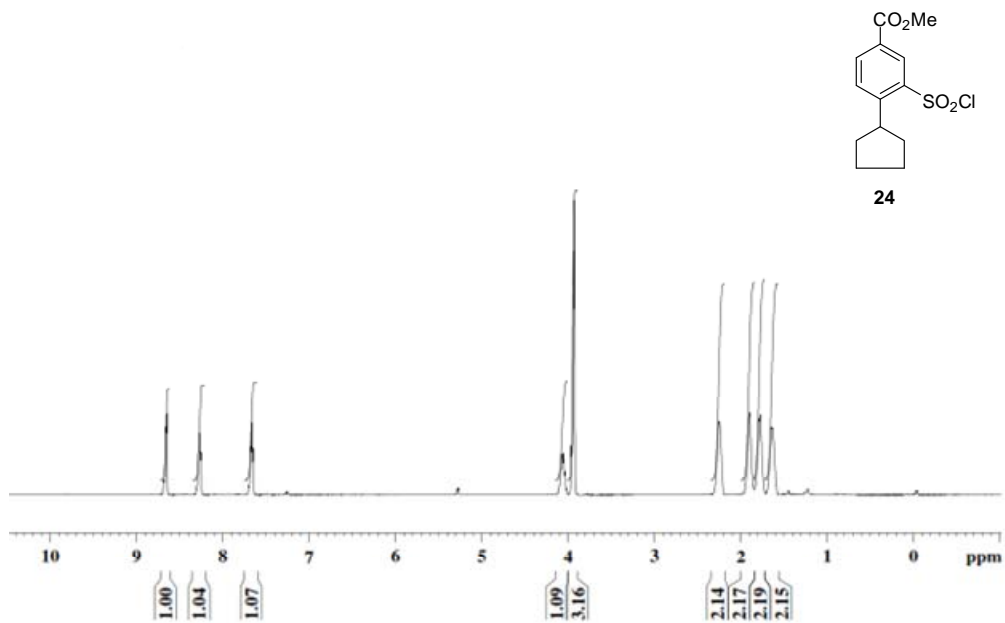
$^{13}\text{C NMR}(\text{CDCl}_3)$ of **17**



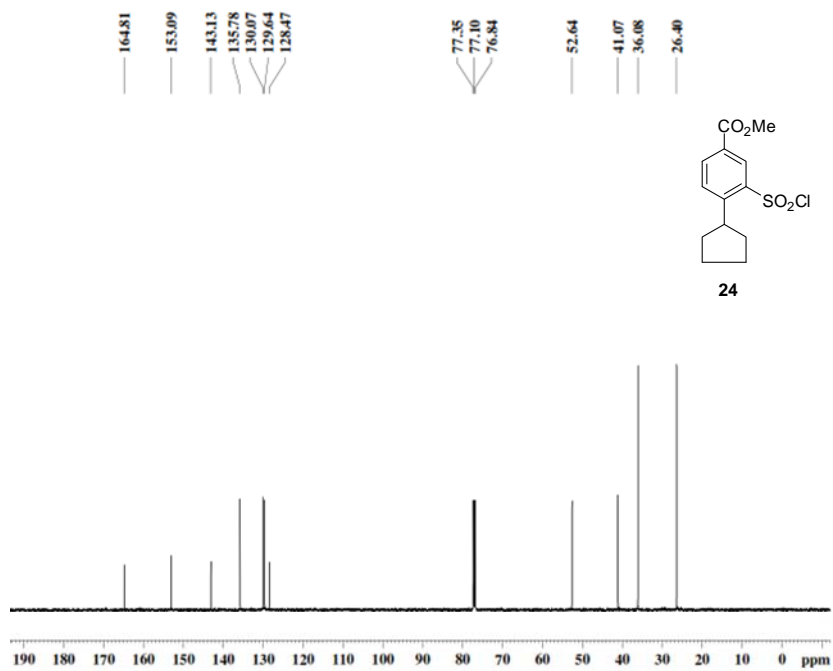
$^1\text{H NMR}(\text{CDCl}_3)$ of **8**



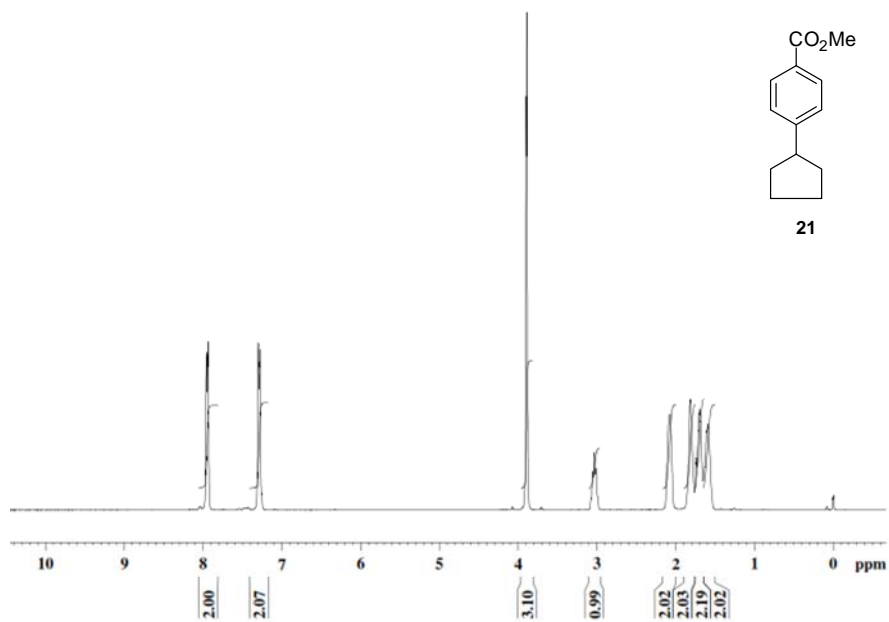
$^{13}\text{C NMR}(\text{CDCl}_3)$ of **8**



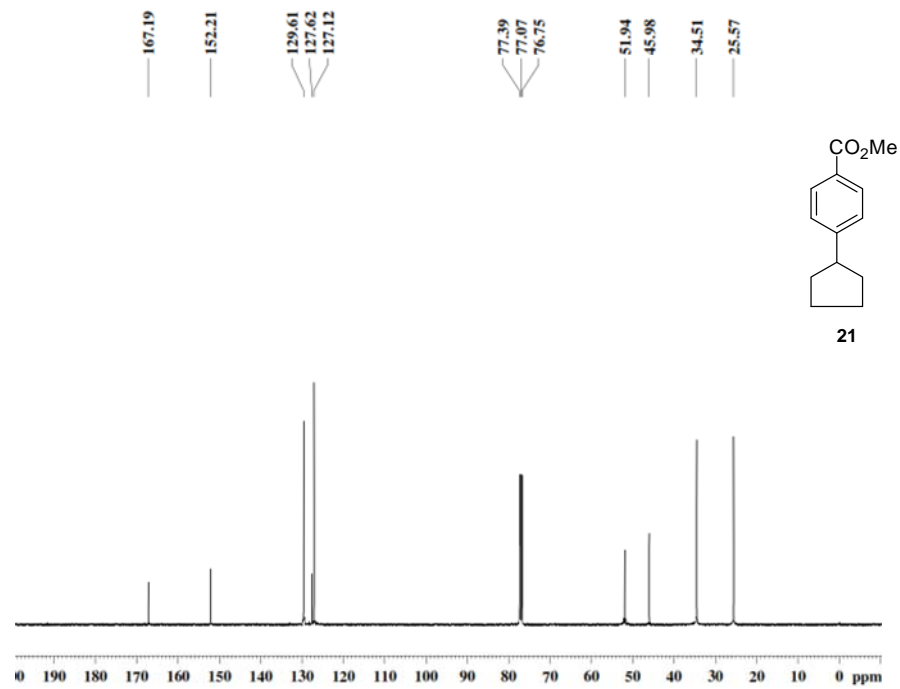
$^1\text{H NMR}(\text{CDCl}_3)$ of **24**



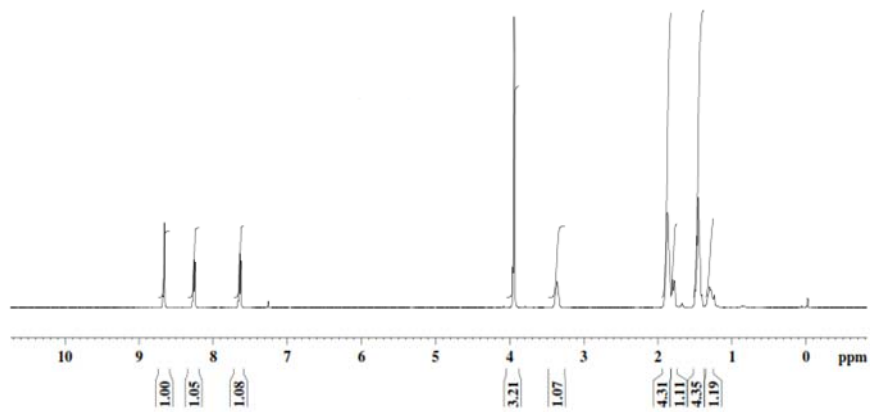
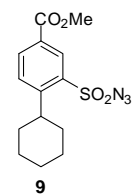
$^{13}\text{C NMR}(\text{CDCl}_3)$ of **24**



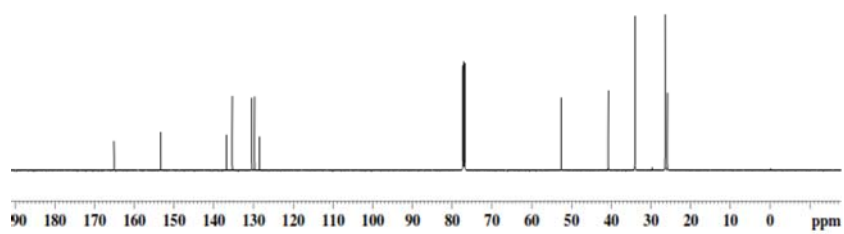
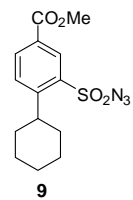
¹H NMR(CDCl₃) of **21**



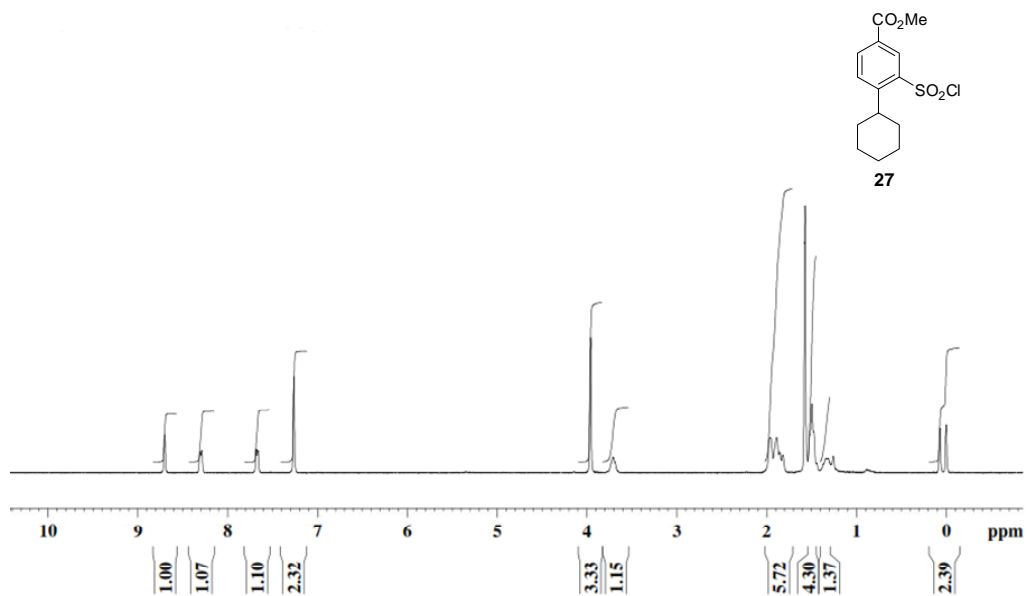
¹³C NMR(CDCl₃) of **21**



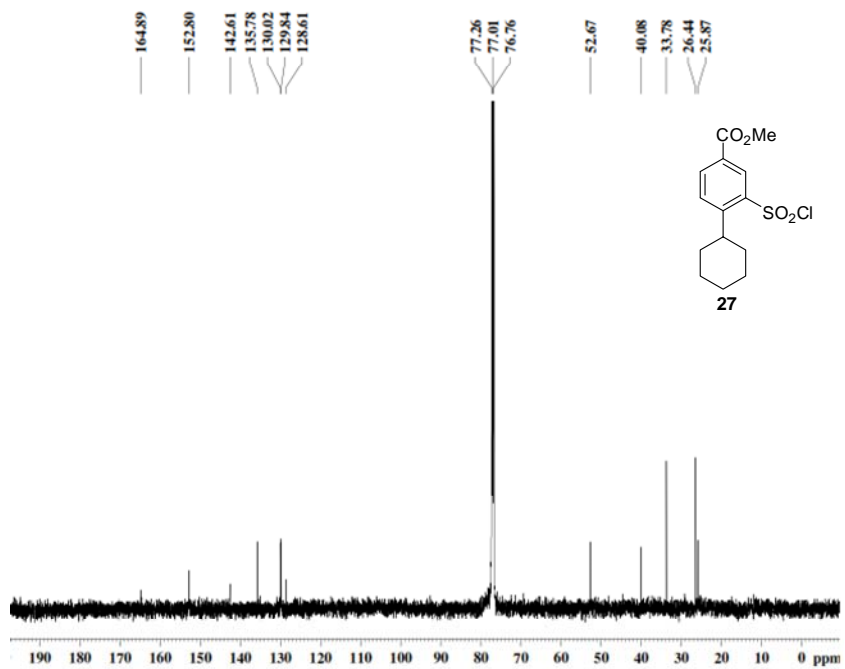
$^1\text{H NMR}(\text{CDCl}_3)$ of **9**



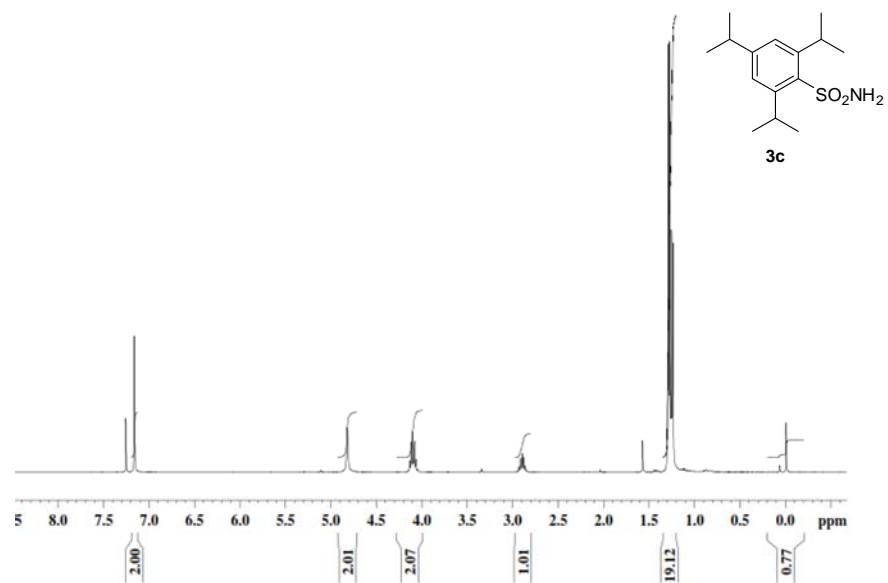
$^{13}\text{C NMR}(\text{CDCl}_3)$ of **9**



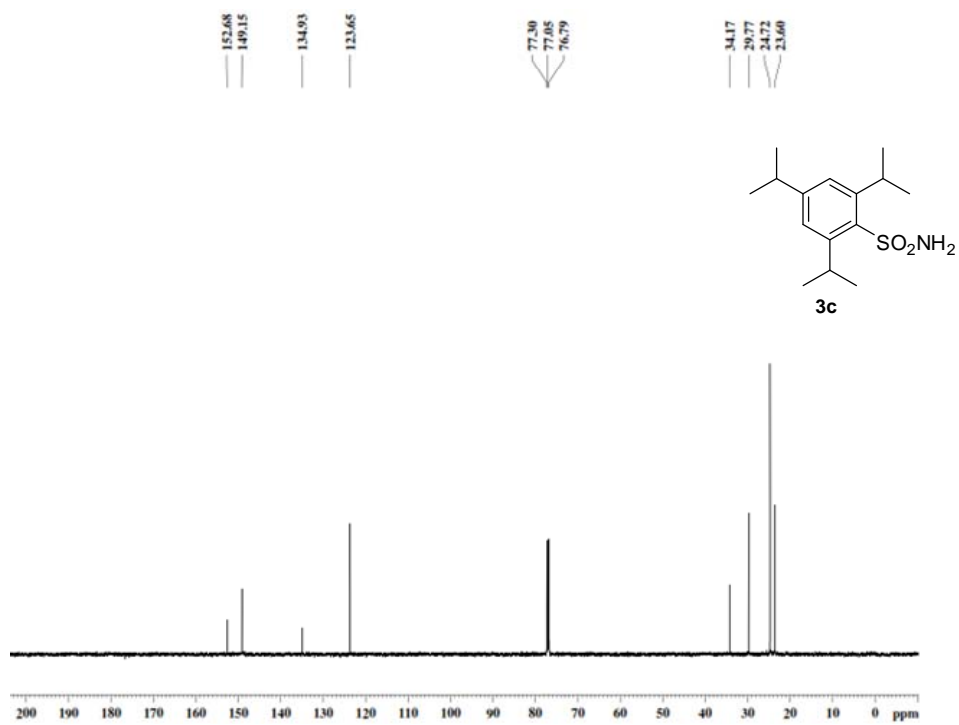
¹H NMR(CDCl₃) of **27**



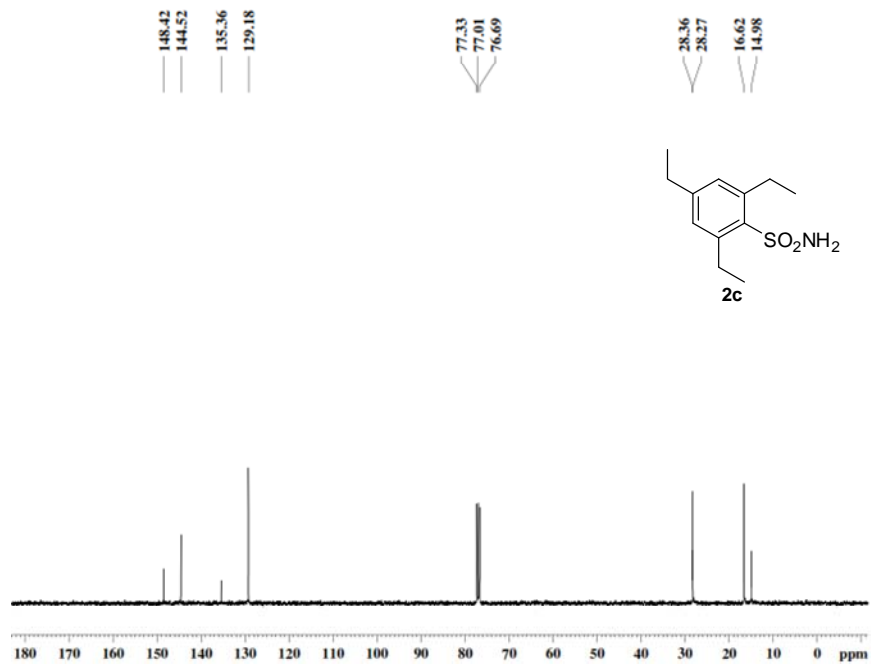
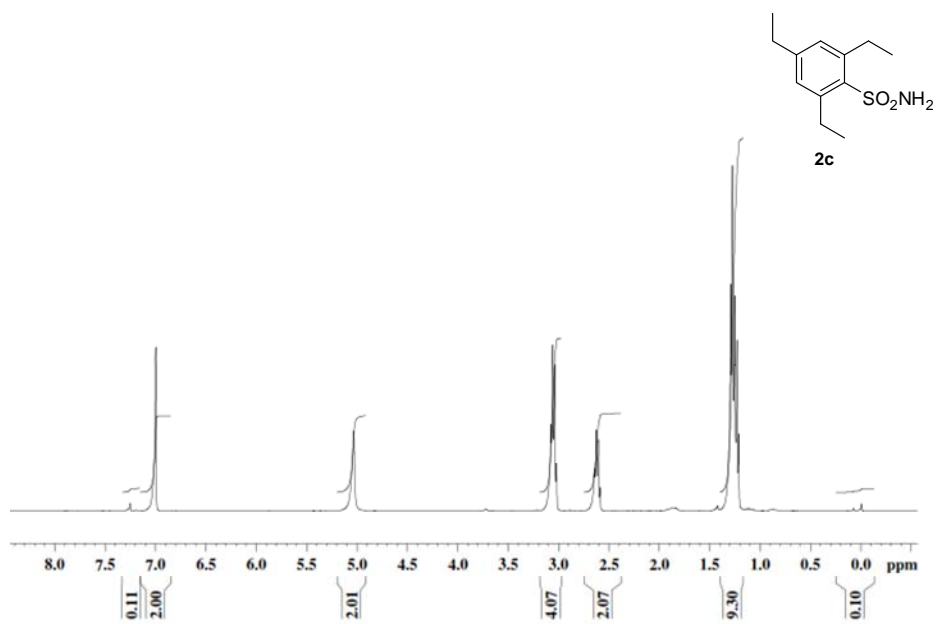
¹³C NMR(CDCl₃) of **27**

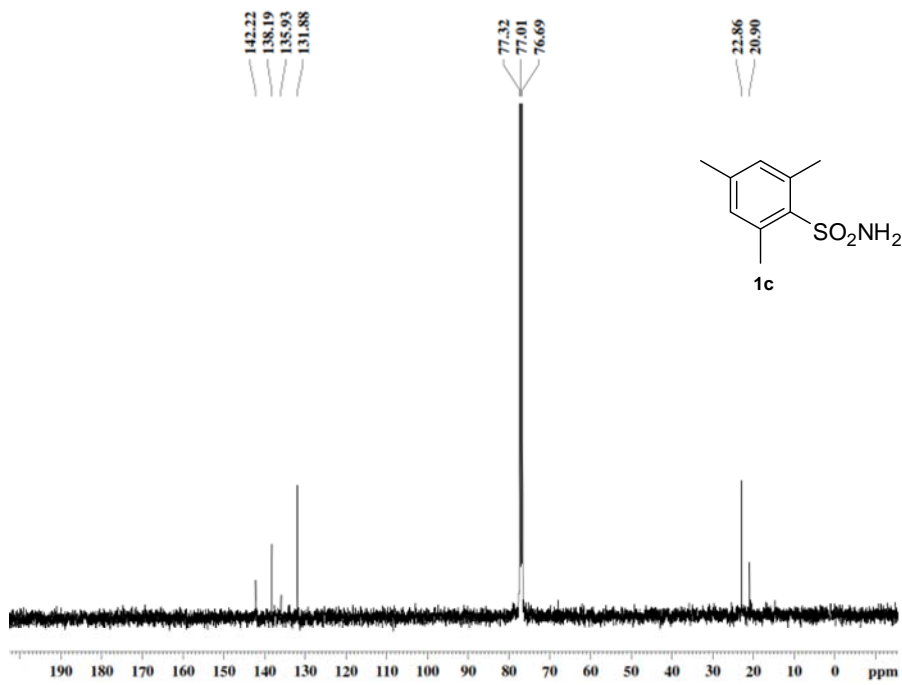
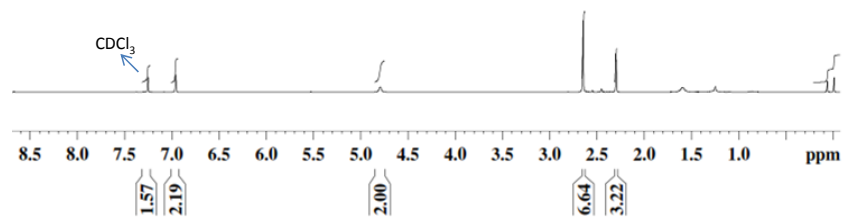
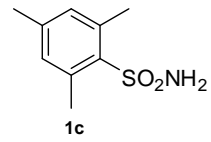


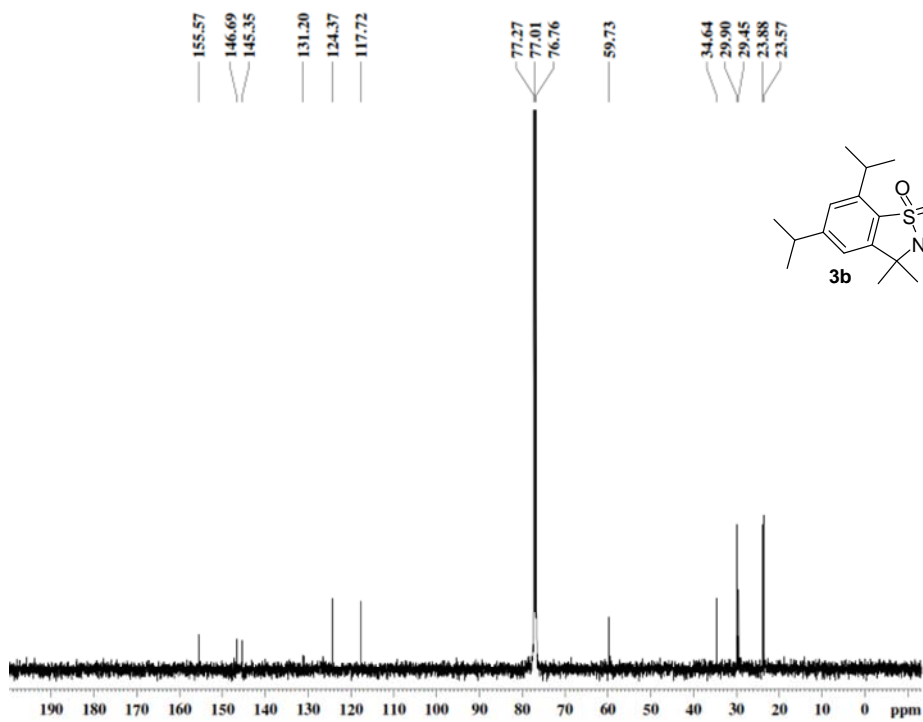
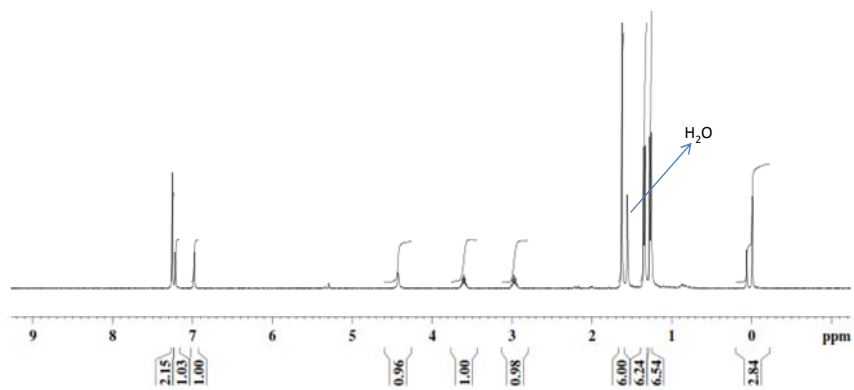
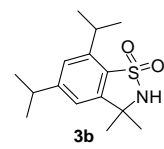
¹H NMR(CDCl₃) of **3c**

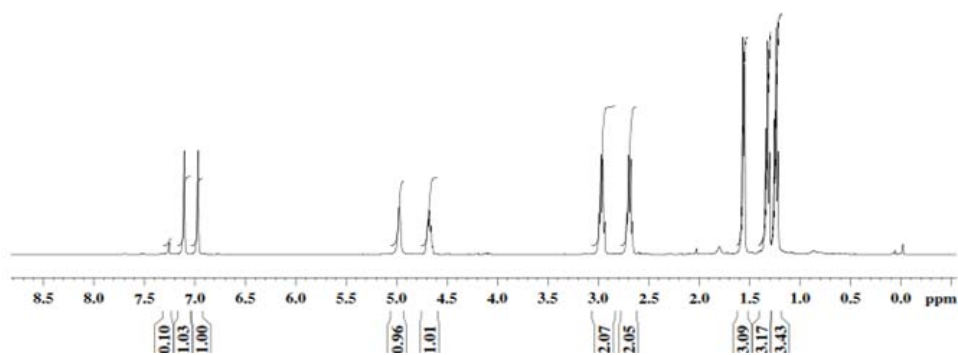
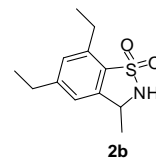


¹³C NMR(CDCl₃) of **3c**

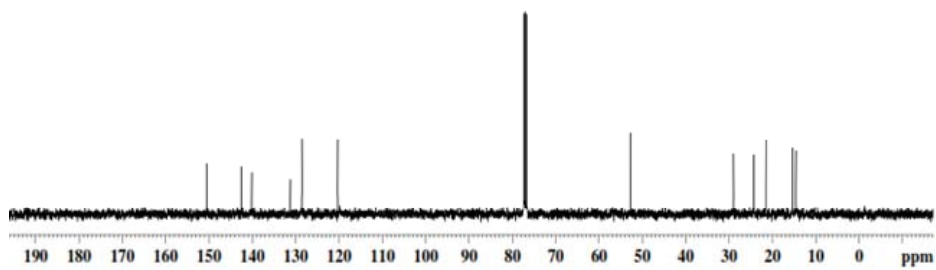
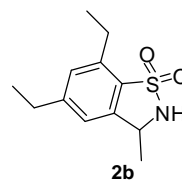
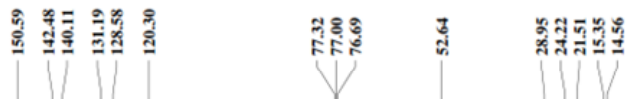




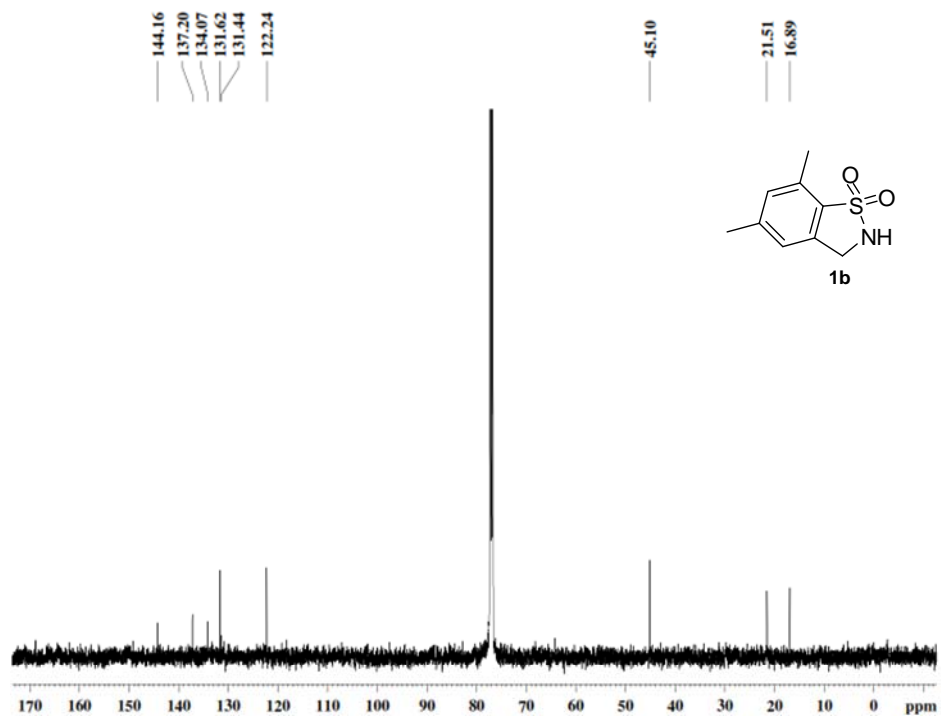
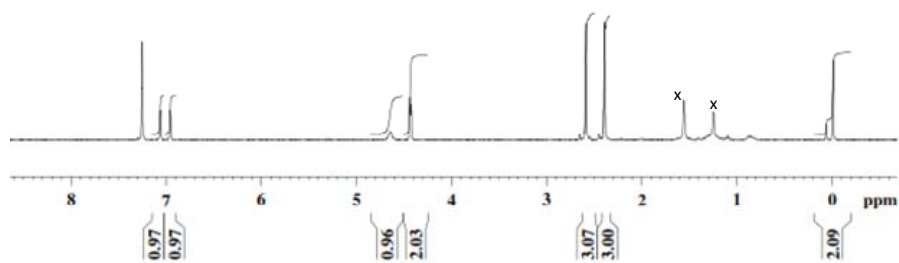
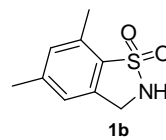


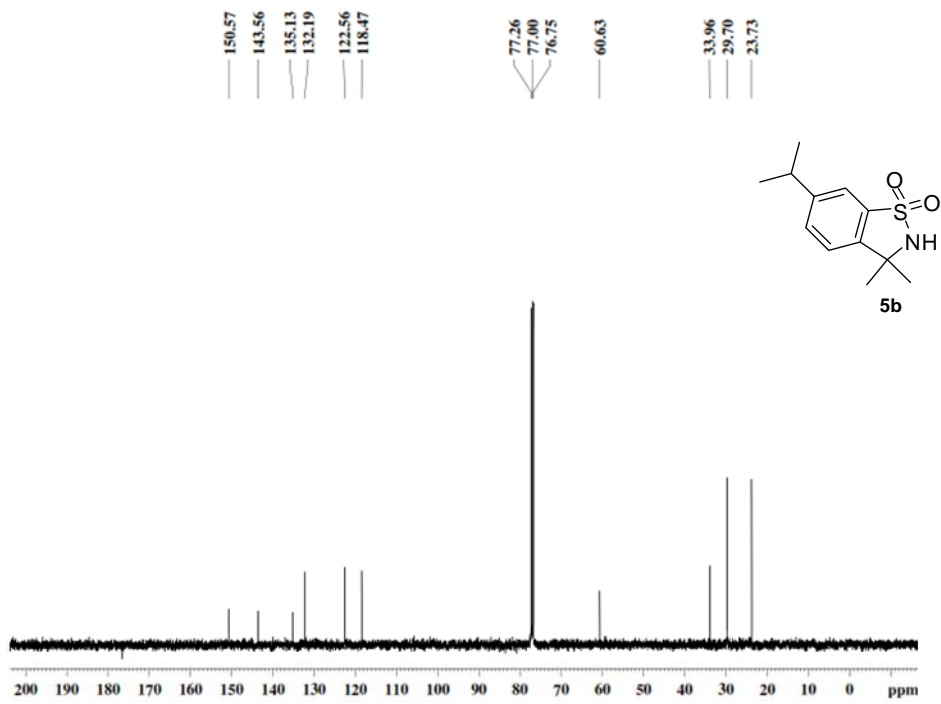
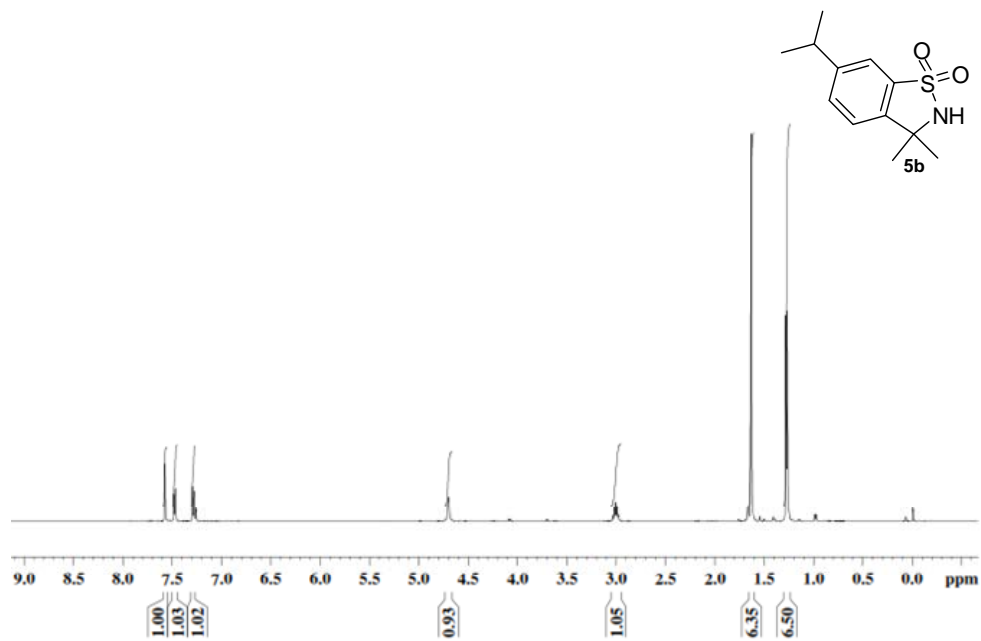


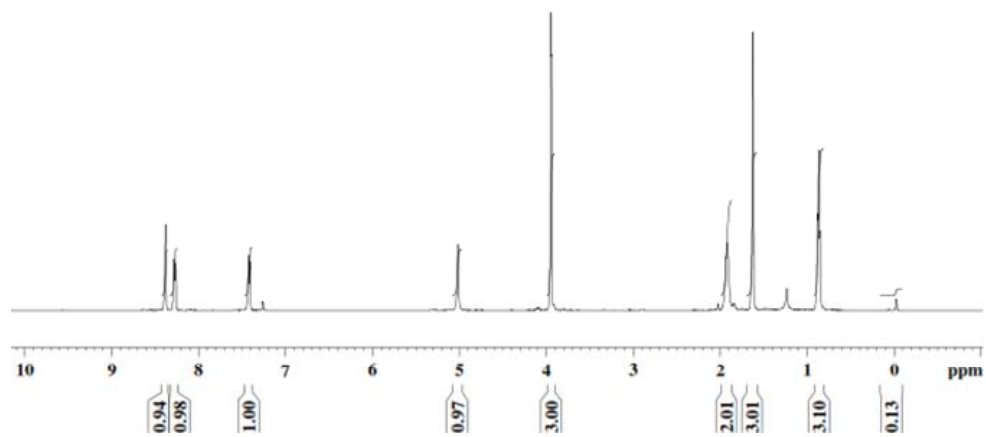
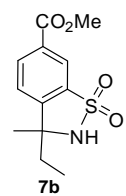
$^1\text{H NMR}(\text{CDCl}_3)$ of **2b**



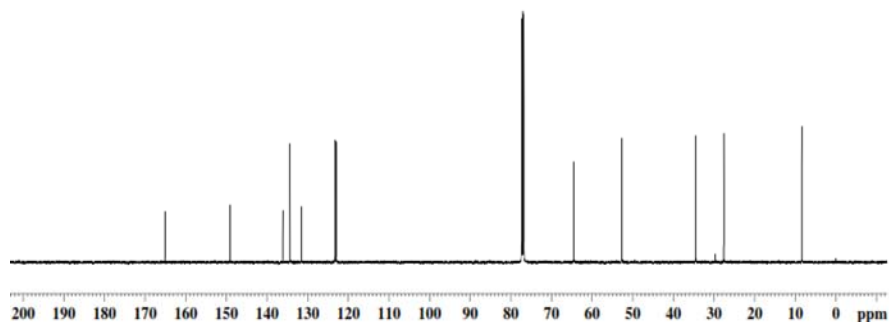
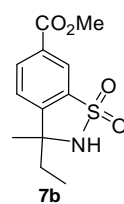
$^{13}\text{C NMR}(\text{CDCl}_3)$ of **2b**



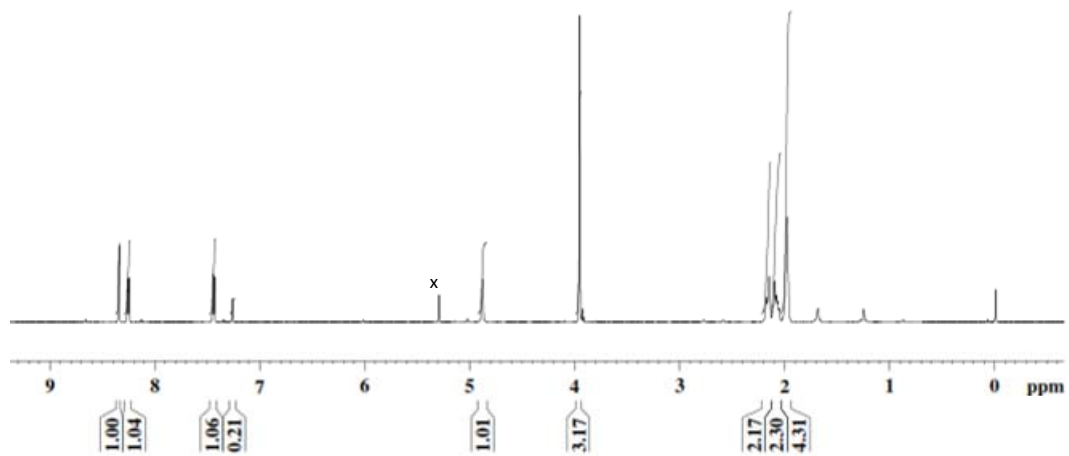
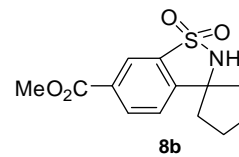




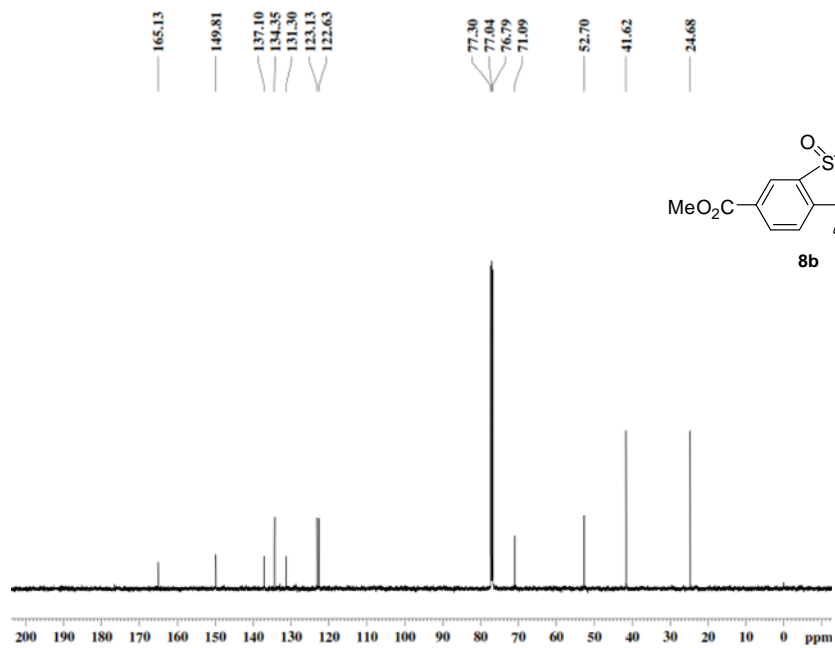
$^1\text{H NMR}(\text{CDCl}_3)$ of **7b**



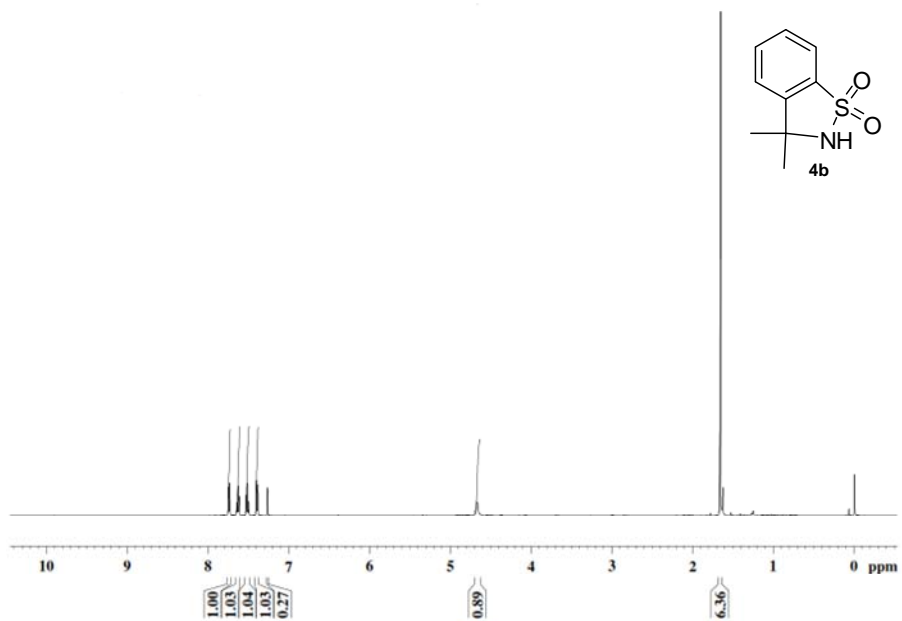
$^{13}\text{C NMR}(\text{CDCl}_3)$ of **7b**



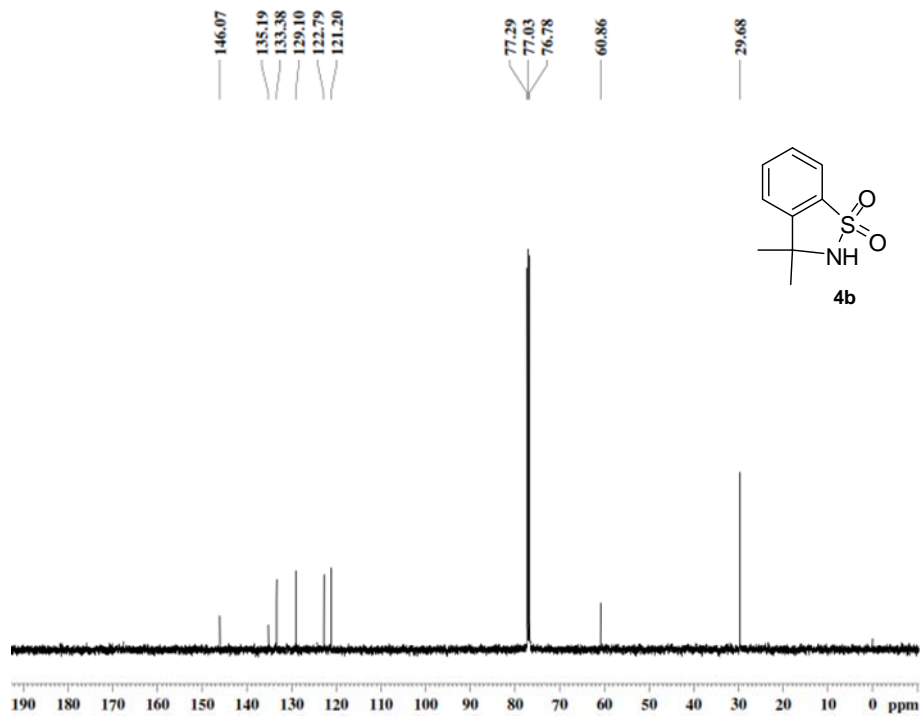
$^1\text{H NMR}(\text{CDCl}_3)$ of **8b**



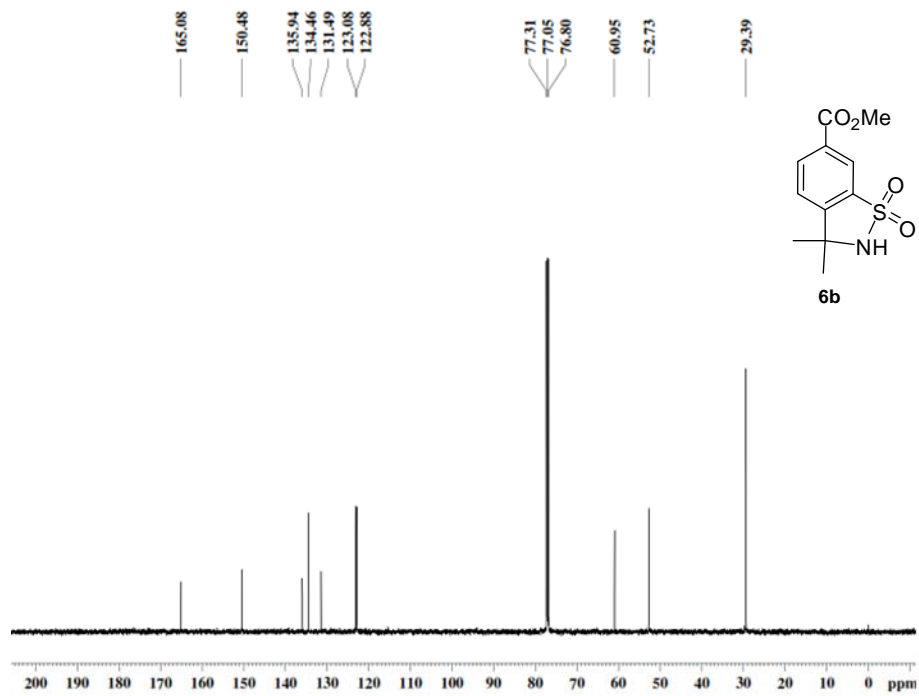
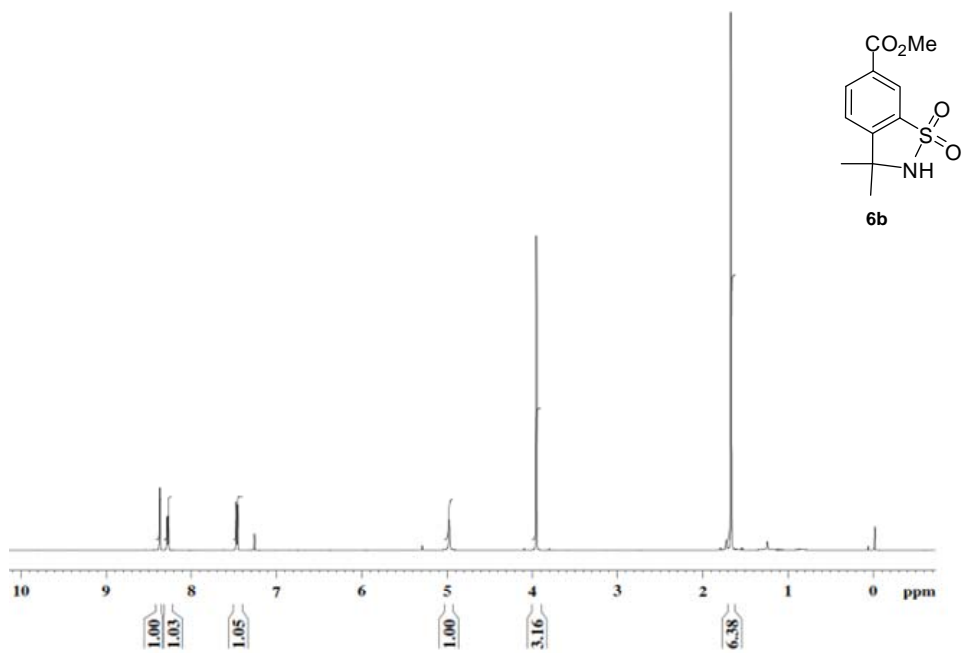
$^{13}\text{C NMR}(\text{CDCl}_3)$ of **8b**

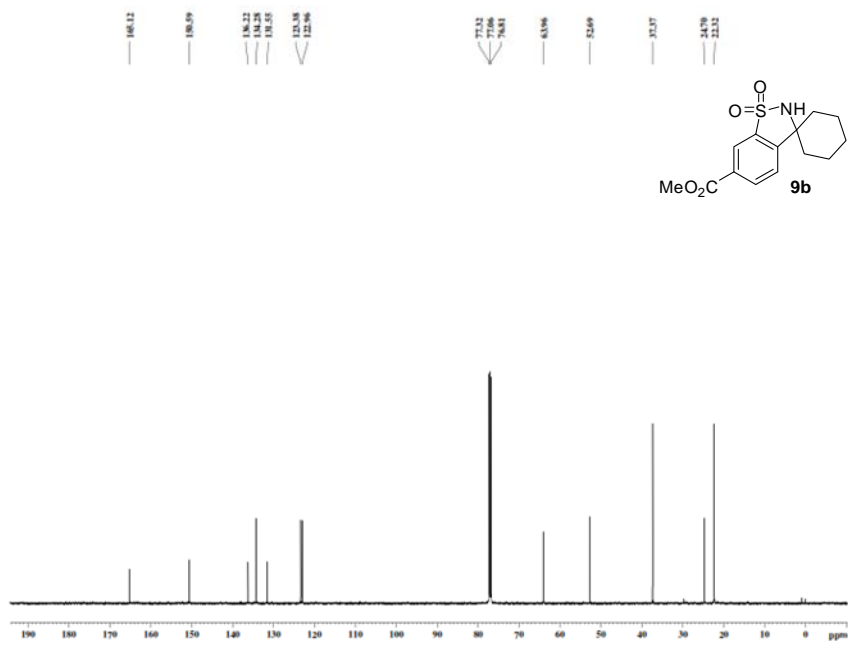
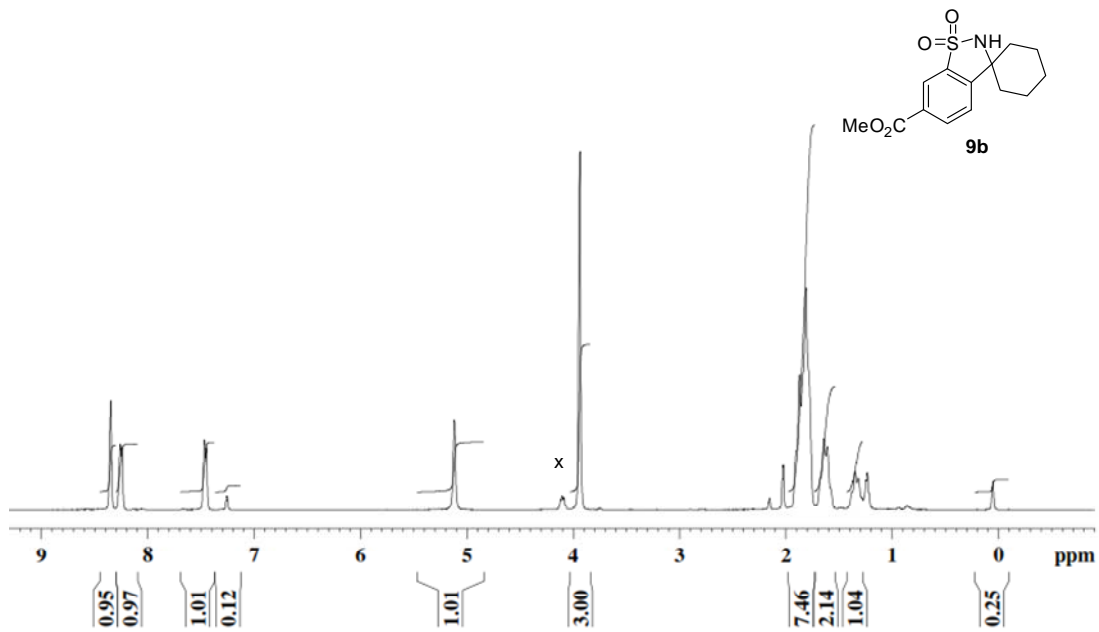


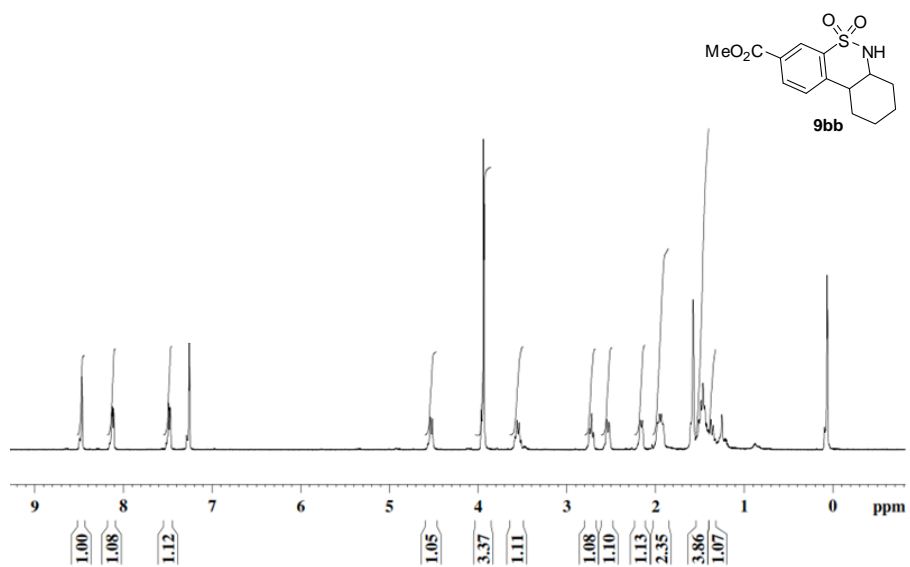
¹H NMR(CDCl₃) of **4b**



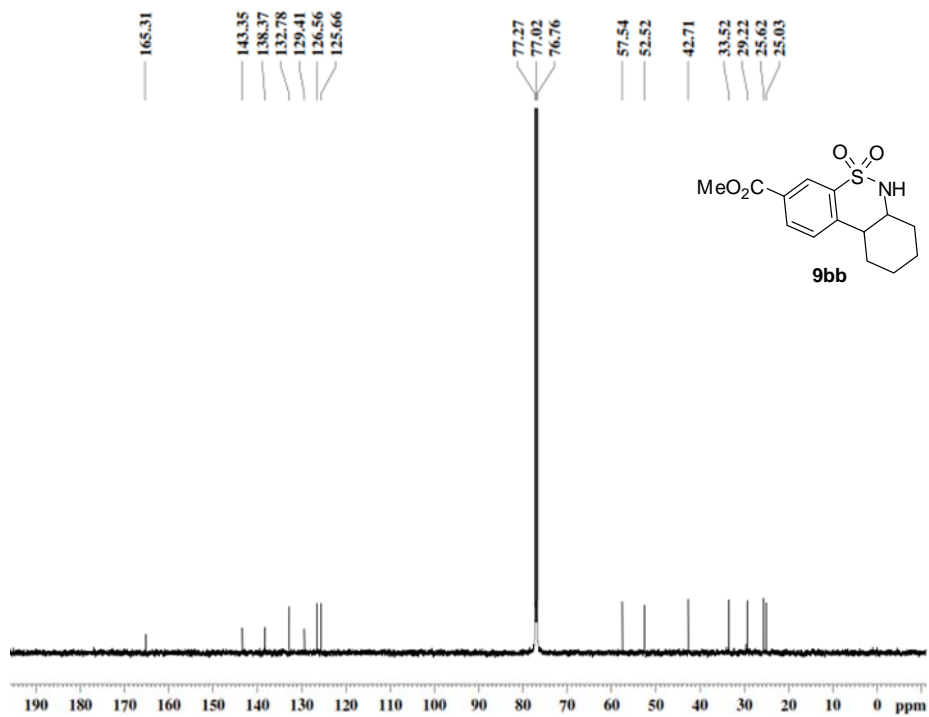
¹³C NMR(CDCl₃) of **4b**







$^1\text{H NMR}(\text{CDCl}_3)$ of **9bb**



$^{13}\text{C NMR}(\text{CDCl}_3)$ of **9bb**

References

- (1) (a) Fasan, R.; Meharena, Y. T.; Snow, C. D.; Poulos, T. L.; Arnold, F. H. *J. Mol. Biol.* **2008**, *383*, 1069; (b) Glieder, A.; Farinas, E. T.; Arnold, F. H. *Nat. Biotechnol.* **2002**, *20*, 1135.
- (2) Peters, M. W.; Meinhold, P.; Glieder, A.; Arnold, F. H. *J Am Chem Soc* **2003**, *125*, 13442.
- (3) Zhang, K.; El Damaty, S.; Fasan, R. *J Am Chem Soc* **2011**, *133*, 3242.
- (4) Ruppel, J. V.; Kamble, R. M.; Zhang, X. P. *Org. Lett.* **2007**, *9*, 4889.
- (5) Fey, N.; Howell, J. A. S.; Lovatt, J. D.; Yates, P. C.; Cunningham, D.; McArdle, P.; Gottlieb, H. E.; Coles, S. J. *Dalton Trans.* **2006**, 5464.
- (6) Kendall, J.; Jackie, D.; Marshall, A. J. **2009**, *PCT Int. Appl. WO 2009008748 A1*.
- (7) Hales, N. J.; Heaney, H.; Hollinshead, J. H.; Ley, S. V. *Tetrahedron* **1995**, *51*, 7741.
- (8) Everson, D. A.; Shrestha, R.; Weix, D. J. *J Am Chem Soc* **2010**, *132*, 3636.